Thallium isotopic compositions in Hawaiian lavas: evidence for recycled materials on the Kea side of the Hawaiian mantle plume

Nicole M.B. Williamson[1], Dominique Weis[1], Julie Prytulak[2]

[1]Pacific Centre for Isotopic and Geochemical Research, Department of Earth, Ocean and Atmospheric Sciences, 2020-2207 Main Mall, University of British Columbia, Vancouver, BC, V6T 1Z4, Canada.

[2]Department of Earth Sciences, Durham University, Durham, DH13LE, UK

Corresponding author e-mail: Nicole Williamson (nwilliam@eoas.ubc.ca)

Key Points:

- Thallium isotopic compositions measured in a sample set of Hawaiian shield lavas represent primary magmatic signatures
- Heavier isotopic values in some Kea-trend volcanoes suggest the presence of ancient pelagic sediment in the Kea source of the Hawaiian plume
- The deep mantle source of both Loa and Kea Hawaiian volcanoes contains recycled materials of varying lithologies, histories, and ages

Abstract

Hawaiian volcanoes record 6 Ma of potentially deep mantle chemistry and form two parallel volcanic chains that are geochemically unique, named Loa and Kea. Loa volcanoes erupt lavas with isotopically enriched compositions thought to reflect the presence of recycled material in the deep mantle source of the Hawaiian plume. Variation in stable thallium (Tl) isotopes have been used to trace recycled pelagic ocean sediment from subduction to eruption in arc and intraplate lavas. Previous work attributed heavy Tl isotopic compositions in eight Loa samples to recycled sediments in their source. We reexamined this hypothesis using a large sample set (n = 34) of shield-stage, tholeiitic basalt from 13 Hawaiian volcanoes representing the entire range of isotopically enriched and depleted compositions along the Hawaiian chain. Samples were acid-leached prior to isotopic analysis to remove post-eruption alteration and resulting ε^{205}Tl values show statistical differences between Loa and Kea volcanoes. Corresponding isotopic data and re-analyzed trace element concentrations suggest that the ε^{205}Tl values are primary magmatic signatures. Possible co-variations between heavy ε^{205}Tl and oxygen isotopes in samples from Kea-trend volcanoes could reflect the presence of ancient, recycled pelagic sediment on the Kea side of the Hawaiian plume, which samples the average deep Pacific mantle. Thus, the deep mantle source of both Loa and Kea Hawaiian volcanoes contains recycled materials of different natures and recycling histories, which supports work from both geophysical and geochemical studies suggesting that the Earth's lower mantle is chemically heterogeneous on multiple spatial scales.

Plain language summary

The Hawaiian volcanoes form two parallel geographic and geochemical trends, named Loa and Kea, that are produced by a deep mantle plume originating at the core-mantle boundary. Volcanoes from the Loa trend have more 'enriched' isotopic compositions, indicative of recycled surface materials in their source, whereas volcanoes from the Kea trend tend to have average Pacific mantle compositions. Thallium (Tl) isotopes (^{205}Tl and ^{203}Tl) are unequally distributed across Earth's chemical reservoirs and can show large concentration contrasts, for example between pelagic sediments (>>100 ng/g) and the Earth's mantle (< 1 ng/g). We measured the Tl isotopic composition in Hawaiian samples and found that, among other indicators, the heavier Tl isotopic compositions measured in some volcanoes of the Kea geochemical trend might co-vary with oxygen isotopes, suggesting that their Tl compositions could result from recycled surface materials in their source. This shows that the mantle source of both the Loa and Kea geochemical trends likely contains materials recycled through the mantle, which is significant because thus far the Kea volcanoes have shown fairly uniform isotopic compositions representative of the average, deep Pacific mantle.

1. Introduction

The Hawaiian-Emperor chain is an ideal natural laboratory for exploring mantle chemical heterogeneity because it records over 80 Ma of potentially deep Pacific mantle chemistry along nearly 6000 km of seamounts and volcanoes created by the long-lived Hawaiian mantle plume (e.g., Tatsumoto, 1978; Regelous et al., 2003; Montelli et al., 2006; Hofmann and Farnetani, 2013; Weis et al., 2011; French and Romanowicz 2015; Harrison et al., 2017; Harrison & Weis, 2018). Hawaiian shield volcanoes are dominated by one of two geochemical compositions that match their geographic distribution; these two geographic and geochemical trends are named Loa and Kea after their largest corresponding volcanoes and have distinct mantle sources constrained and identified by their respective isotopic compositions (Jackson et al., 1972; Tatsumoto, 1978;

Abouchami et al., 2005; Weis et al., 2011; Weis et al., 2020) (Figure 1). The compositions of shield lavas from Loa-trend volcanoes are higher in $^{208}Pb^*/^{206}Pb^*$ and $^{87}Sr/^{86}Sr$ (higher time-integrated Th/U and Rb in the original source) and trend towards the Enriched Mantle I (EM-1) mantle component (e.g., Abouchami et al., 2005; Fekiacova et al., 2007; Hoffman, 2014; White, 2015), which is hypothesized to include material from foundered subcontinental lithosphere, 1-2 Ga pelagic sediment, or lower continental crust (e.g., Hofmann, 2014). The source of enriched compositions measured in Loa-trend lavas may originate from the Pacific Large Low Shear Velocity Province (LLSVP; Bower et al., 2013) and/or ultra-low velocity zone (ULVZ; McNamara et al., 2010; Li et al., 2017), both located to the southwest of the Hawaiian Islands near the core-mantle boundary (CMB) (e.g., Harrison et al., 2017). In contrast, shield lavas from Kea-trend volcanoes have lower $^{208}Pb/^{204}Pb$ for a given $^{206}Pb/^{204}Pb$, lower time-integrated Th/U ($^{208}Pb^*/^{206}Pb^*$), and lower $^{87}Sr/^{86}Sr$ (Abouchami et al., 2005; Weis et al., 2011; Nobre Silva et al., 2013) and thus are typically thought to represent the average deep Pacific mantle (i.e., PREMA; White, 1985; Zindler and Hart, 1986) sampled from a source outside the LLSVP to the northeast of Hawai‘i (Weis et al., 2011, Harrison et al., 2017). However, recent work has identified three, statistically different radiogenic isotopic subgroups within the Kea geochemical group (‘Transitional Kea’, ‘Kohala’, and ‘Kea’; Weis et al., 2020), suggesting that smaller-scale mantle heterogeneities are present within the Kea source (e.g., Eisele et al., 2003; Greene et al., 2013; Pietruszka et al., 2018) and that the average deep Pacific mantle may be more heterogeneous than previously thought (Starkey et al., 2016; Torsvik et al., 2016; Parai et al., 2019; Harpp and Weis, 2020; Mundl-Petermeier et al., 2020; Weis et al., 2020).

Stable isotope systematics of elements such as thallium (Tl), have been used to assess the presence and lithological origin of recycled surface materials in ocean island basalts (OIB) (e.g., Nielsen et al., 2006b; Nielsen et al., 2007; Prytulak et al., 2017; Blusztajn et al., 2018; Brett et al., 2021). The two stable isotopes of Tl, ^{205}Tl and ^{203}Tl, are fractionated between Earth’s geochemical reservoirs by more than 35 epsilon (x 10 000) units. Furthermore, Tl concentrations between reservoirs may vary by up to six orders of magnitude (see review in Nielsen et al., 2017a). Average MORB has an $\varepsilon^{205}Tl$ of -2.0 ± 0.5 (2SD) and is used as the inferred isotopic composition of the MORB mantle, given the lack of evidence for Tl isotopic fractionation during partial melting (Nielsen et al., 2017a and references therein). Pelagic sediments typically have isotopically heavy $\varepsilon^{205}Tl$ values (+3 to +5; Rehkämper et al., 2002) because they are rich in manganese (Mn) oxides, which preferentially adsorb the heavy isotope (^{205}Tl) onto their surfaces (Peacock and Moon, 2012; Nielsen et al., 2013). Conversely, low-temperature altered oceanic crust (AOC) is isotopically light, with an $\varepsilon^{205}Tl$ as low as -15, due to the addition of light Tl from seawater that permeates into the upper crust (Nielsen et al., 2006a). The potential utility of Tl as a mantle source tracer is enhanced by the fact that Tl isotopes are not typically fractionated during magmatic processes, such as fractional crystallization (Prytulak et al., 2017; Gaschnig et al., 2021) and partial melting, as assessed by comparison of MORB and mantle samples (Nielsen et al., 2006b, Nielsen et al., 2015; Fitzpayne et al., 2020), and thus should retain a primary source composition.

The first application of Tl isotopic compositions as a tracer of recycled materials in OIB evaluated picritic basaltic rocks from six Hawaiian volcanoes (Nielsen et al. 2006b). Isotopically heavy $\varepsilon^{205}Tl$ compared to MORB was measured in a number of the samples and attributed to the presence of recycled ferromanganese-rich pelagic sediments in the Hawaiian source (Nielsen et al., 2006b). We revisit and expand upon this hypothesis with a high-density sample set of

tholeiitic, shield-stage Hawaiian lavas (n = 34) specifically selected to span the full range of radiogenic isotopic compositions occurring along as much of the Hawaiian Islands as possible (Figure 1). We tested and employed a leaching protocol to remove post-eruption alteration, which is recognized to contribute erroneous values to both radiogenic (Abouchami et al., 2000; Hanano et al., 2009; Nobre Silva et al., 2009) and stable (Harrison et al., 2015; Nielsen et al., 2016) isotopic compositions. Removal of post-eruption alteration is especially important for submarine Hawaiian samples, as these are likely to accumulate post-eruptive Fe-Mn crusts (Craig et al., 1982; Hein and Koschinsky, 2014) with very high Tl concentrations compared to the lavas and potentially heavy ε^{205}Tl values (e.g., Nielsen et al., 2016). We compared the measured ε^{205}Tl values to radiogenic isotopes of Pb, Sr, Nd, and Hf and predicted that samples from Loa-trend volcanoes, with their 'enriched' radiogenic isotopic compositions, would also have isotopically heavy ε^{205}Tl values. This prediction was made given that the 'enriched' isotopic compositions measured in Loa shield lavas are thought to originate from the presence of recycled surface materials into the deep mantle source (e.g., Weis et al., 2011). However, we obtained the opposite result, with the Kea-trend volcanoes yielding the heaviest ε^{205}Tl values. The samples chosen for this study are geochemically well-characterized; thus we were able to integrate a number of other isotopic systems (Pb, Sr, Nd, Hf, O) and trace element discriminants such as Ce/Tl, Cs/Tl, Rb/Cs, and Th/Tl, to both assess the influence of syn- and post-eruptive processes on the Tl isotopic compositions of the samples (e.g., Nielsen et al., 2017b and references therein; Brett et al., 2021) and to explore the implications for the origin of heterogeneities in the deep mantle source of the Hawaiian mantle plume.

2. Samples and analytical procedure

Recent Hawaiian volcanoes (i.e., those that form the emergent islands, from 6 to 0 Ma; Figure 1) are ideal for studying the nature of mantle heterogeneities due to a large existing sample set (compared to other volcanic island chains) that is geochemically well-characterized (e.g., n > 800 for Pb isotopes, Weis et al., 2020). The samples used in this study (n = 34 from 13 volcanoes), were chosen on the basis of their high-precision radiogenic isotopic compositions (e.g., ^{206}Pb/^{204}Pb, ^{207}Pb/^{204}Pb, ^{208}Pb/^{204}Pb, ^{87}Sr/^{86}Sr, ^{143}Nd/^{144}Nd, and ^{176}Hf/^{177}Hf; isotopic database can be found in the supporting information of Weis et al., 2020) and geographic locations, from Kaua'i (5-6 Ma) to Lō'ihi (0 Ma), with the goal of representing the full range of isotopic end-member compositions observed along the Hawaiian Islands (Figure 1). This approach allows for a comprehensive comparison of the ε^{205}Tl between Hawaiian volcanoes with isotopically depleted and enriched lavas, i.e., those of the Kea and Loa geochemical trends, and by extension OIB formed from PREMA and EM-1-like sources, as well as those from the six geochemical subgroups recently identified by Weis et al. (2020). This study is the highest sample density investigation of Tl isotopes on a single oceanic chain and deliberately features a mix of submarine and subaerial tholeiitic basalts from the shield-building volcanic stage of each volcano, including Lō'ihi (n = 2), Kīlauea (n = 4), Mauna Loa (n = 4), Mauna Kea (n = 4), Hualālai (n = 2), Kohala (n = 1), Hāna Ridge (submarine Haleakalā (Ren et al., 2004); n = 2), West Maui (n = 5), Ko'olau (n = 4), Wai'anae (n = 1), West Ka'ena (n = 3), and Kaua'i (n = 2) (supporting information Table S1). Shield-stage basalts represent >95% of a Hawaiian volcano's erupted volume and are formed from the highest-degree partial melts generated in the central, hottest part of the mantle plume (e.g., DePaolo et al., 2001). Thus, they best represent the bulk chemistry and mantle source of each volcano (e.g., Hanano et al., 2010).

All chemical and analytical procedures were carried out at the Pacific Centre for Isotopic and Geochemical Research (PCIGR) at the University of British Columbia, Vancouver, Canada. Chemical and analytical methods were first tested on 5 reference materials (Table 1). Samples were screened for signs of alteration on the basis of their pre-existing major and trace element data (e.g., loss-on-ignition < 2 wt%) and physical appearance or on descriptions in the literature when a hand sample was not available. Samples that required physical processing were cut and crushed in a Rocklabs® tungsten-carbide hydraulic press and powdered using an agate planetary mill. Most samples had existing published radiogenic isotopic compositions and major and trace element concentrations; however, for internal consistency, samples were re-run for 41 trace element concentrations, including thallium. Nine samples that did not have published major element data were analyzed by ICP-OES and XRF according to methods outlined in Carpentier et al. (2013) and Rhodes and Vollinger (2004), respectively (Table S1). In addition, eight recently acquired samples that did not have any published Pb, Sr, Nd, and Hf isotopic compositions were processed and analyzed according to methods outlined in Fourny et al. (2016). The supporting Table S1 includes all isotopic, trace element, and major element data as well as relevant data reproducibility information and sources.

2.1 Trace element analyses

Trace element concentrations were collected for all 34 samples and five reference materials on unleached (n = 44), leached (n = 9), and leachate (n = 8) aliquots, including duplicates. Trace elements measured from the leached and leachate aliquots were only used in the leaching experiment: for full details see supporting information Text S1. Chemical preparation for trace element analysis follows the procedures outlined in Fourny et al. (2016). Briefly, approximately 100 mg of powder was digested on a hotplate using an HNO_3-HF mix, diluted 5000 times, and concentrations were measured using a Thermo Finnigan Element2 high-resolution inductively-coupled mass spectrometer (HR-ICP-MS) that was calibrated with values from the USGS standard BCR-2 as reported in Fourny et al. (2016) and a thallium concentration of 306 ng/g as reported in Brett et al. (2018). Measured values were corrected offline using a standard-sample bracketing method with repeated analyses of BCR-2. Total procedural duplicates (n = 5) and analytical replicates (n = 18) were in good agreement (RSDs < 5-10%) while total procedural blanks (n = 4) had Tl concentrations below the detection limit (< ~0.0003 μg/g). The USGS reference materials BCR-2 (Columbia River basalt; n = 18 analyses) and BHVO-2 (Hawaiian tholeiitic basalt; n = 4) and the PCIGR in-house reference material KIL-93 (Hawaiian tholeiitic basalt; n = 16) were measured during multiple analytical sessions and showed reproducible results, with RSDs less than 10% for the majority of trace elements and good agreement with published values (Table S1) (Frey et al., 1994; Govindaraju, 1994; Eggins et al., 1997; Wilson, 1997; Norman and Garcia, 1999; Weis et al., 2005; Schudel et al., 2015; Fourny et al., 2016). Thallium concentrations measured for BHVO-1, BHVO-2, and BCR-2, are within 5% of values reported in the literature (Brett et al., 2018; Shu et al., 2017). The two in-house Hawaiian basalt reference materials KIL-93 (from Kīlauea volcano) and KOOLAU (from Koʻolau volcano) had not previously been analyzed for Tl concentrations; their measured values are within the range of samples from the same volcanoes reported in Nielsen et al. (2006).

2.2 Thallium isotopic analyses

Thallium isotopes were analyzed for all 34 Hawaiian samples and 5 reference materials on leached (n = 44) and unleached (n = 21) aliquots, including duplicates. In addition, a test was performed on reference materials centrifuged before column loading to remove a precipitate

formed as the result of digestion (n = 6, including a duplicate) – similar to findings of Nielsen et al. (2005), the centrifuged and uncentrifuged reference materials yielded identical ε^{205}Tl values, within error (see Table S1 for data and Text S1for explanation).

All samples were acid leached prior to column chemistry, except when performing the leaching experiment (details in Text S1). The leaching procedure follows the cold leaching method outlined in Weis et al. (2006) and Nobre Silva et al. (2009). Aliquots of 0.1 to 2 g of sample powder were weighed prior to leaching, depending on the Tl concentration of the sample. When over 0.3 to 0.5 g of sample was necessary, the powder was divided into multiple aliquots, which were individually leached, digested, and then recombined onto the columns. For leaching, approximately 10 ml of hydrochloric acid (6 M) was added to the sample powder in a Savillex beaker and then sonicated for twenty minutes to dissolve secondary phases. The sample was then removed and immediately decanted to remove the leachate fraction containing the alteration products. This procedure was repeated until a clear leachate solution was obtained after sonication, indicating that most secondary phases had been removed.

Digestion and column chromatography followed the procedures outlined in Brett et al. (2018), which are modified from the original protocol of Rehkämper and Halliday (1999). Thallium isotopic compositions were measured on a *Nu Plasma* MC-ICP-MS (Nu 21), using on-peak background corrections, integration time of 5s, and a single 60 cycle block. Measured values are reported relative to the Tl standard NIST SRM 997, as follows:

$$\varepsilon^{205}Tl_{SRM997} = \frac{{}^{205}Tl/{}^{203}Tl_{sample} - {}^{205}Tl/{}^{203}Tl_{SRM997}}{{}^{205}Tl/{}^{203}Tl_{SRM997}} \times 10000.$$

Instrument mass fractionation was accounted for by adding the Pb standard solution NIST SRM 981 to the samples prior to analysis and by using an online exponential law correction to the values of ^{208}Pb/^{206}Pb from Galer and Abouchami (1998). When the concentration of Tl in the sample aliquot was high enough, each sample was measured three times. Bracketing standards were prepared to match the samples' intensity and Pb/Tl and the ε^{205}Tl for each individual measurement was calculated using its measured ^{205}Tl/^{203}Tl and the average of its corresponding bracketing standards. The final ε^{205}Tl for each sample or reference material is the average of individual ε^{205}Tl values. When samples could be measured more than two times, the reported uncertainty (2SD) is the standard deviation of the mean. For samples with very low Tl concentrations that could only be analyzed once or twice, the long-term average reproducibility of leached reference materials is assigned (2SD of ± 0.4), as per literature convention (e.g., Brett et al., 2018). Two Tl standards were used to bracket the samples and to test and calibrate the instrument: bracketing standard NIST SRM 997 and the community Aldrich standard, which has been measured over the past decade in numerous labs (e.g., Brett et al. 2018 and references therein). During the course of this study, the average ^{205}Tl/^{203}Tl obtained for SRM 997 was 2.38913 ± 0.00040 with an RSD of 167 ppm (n = 609). Average ^{205}Tl/^{203}Tl obtained for the Aldrich standard is 2.38894 ± 0.00037 with an RSD of 154 ppm (n = 100). The final average ε^{205}Tl obtained for Aldrich is -0.8 ± 0.2 (2SD), which is within error of the average obtained in previous studies (e.g., Brett et al. 2018). Throughout the study, reference material BCR-2 was

measured repeatedly (n = 33) to assess accuracy. The final average ε^{205}Tl obtained for BCR-2 is -2.4 ± 0.4 (2SD), which matches the published value of -2.5 ± 0.5 (2SD) (e.g., Brett et al. 2018). The two other common reference materials used in the literature, BHVO-1 and BHVO-2, yielded ε^{205}Tl values of -3.6 ± 1.0 (2SD) and -1.3 ± 0.5 (2SD), respectively, which are also in agreement with previous values of -3.6 ± 0.4 (2SD) and -1.2 ± 0.7 (2SD) (Shu et al., 2017 and Brett et al., 2018). The two in-house Hawaiian reference materials KIL-93 and KOOLAU yielded ε^{205}Tl values of -1.9 ± 1.0 and -1.7 ± 1.0 (Table 1), which are comparable to the values previously obtained for these volcanoes in Nielsen et al. (2006b). Unless specified, reference materials were not leached to ensure comparability with literature values.

Prior to the isotopic analyses, total procedural blanks (n = 6) were tested for Tl and Pb concentrations according to the method in Brett et al. (2018). All blanks were below detection on the MC-ICP-MS and thus contained <1 pg Pb and Tl. In addition, prior to addition of the Pb standard, all sample aliquots were tested for their Pb concentrations because additional Pb in the aliquot matrix can yield unsystematic errors in mass bias that require subsequent corrections (Brett et al., 2018 and references therein); Pb contents in all purified sample aliquots were below the detection limit and thus contained < 1 pg Pb. Total procedural duplicates and analytical replicates were used throughout the study for both leached and non-leached samples and reference materials (Table 1, 2, and S1). All duplicate and replicate analyses are within error (2SD ε^{205}Tl) and have ^{205}Tl/^{203}Tl RSDs < 49 ppm (average is 20 ppm). The only exception is one leached reference material, KIL-93 L, for which the duplicate is 0.1 epsilon units outside of error (^{205}Tl/^{203}Tl RSD = 58 ppm).

3. Results

Thallium isotopic compositions and relevant trace element concentrations for the Hawaiian samples analyzed are reported in Table 2. Thallium concentrations vary between 7 and 38 ng/g with the exception of one sample from the West Ka'ena Ridge and one sample from the Hāna Ridge (submarine Haleakalā), which have elevated thallium concentrations of 87 and 263 ng/g, respectively (Table 2, Figure 2a). There is no systematic difference in Tl concentration between Loa-trend and Kea-trend volcanoes. Importantly, SiO_2, Na_2O+K_2O, Nb/Y, and Zr/Y values confirm that all samples measured are shield-stage, tholeiitic basalts (supporting information Figure S1).

The ε^{205}Tl values measured for leached Hawaiian shield lavas range from -2.8 ± 0.2 to 4.0 ± 0.4 and there are no correlations between ε^{205}Tl and sampling environment (submarine or subaerial) or age/distance from Kīlauea. Most of the Hawaiian samples have an ε^{205}Tl below 0 and close to the inferred mantle range of -2.0 ± 0.5 (2SD) (Nielsen et al., 2017a and references therein), with the exception of 4 samples from the Kea-trend volcanoes that have positive ε^{205}Tl values: two samples from West Maui (subaerially erupted core samples; 01-MA-1020 and 01-MA-560; ε^{205}Tl of 0.9 ± 0.2 and 1.8 ± 0.2), one from the Hāna Ridge (submarine Haleakalā; K212-8; 2.0 ± 0.4), and one from west Kaua'i (subaerial; KAU-2015-026; 4.0 ± 0.4) (Figure 2a). Samples of Kea-trend volcanoes span the entire range of measured Hawaiian values, whereas samples of Loa-trend volcanoes have a more restricted range of -2.6 ± 0.4 to -1.2 ± 0.4 (Table 2, Figure 2a).

Although the addition of <<1% by mass of Fe-Mn materials can cause a resolvable change in the ε^{205}Tl value of a lava (Nielsen et al., 2017b), it is unlikely that the presence of post-

eruptive Fe-Mn crusts on the samples is responsible for the anomalously heavy ε^{205}Tl values because this study (see Text S1) and previous work (e.g., Nielsen et al., 2017b) have demonstrated that post-eruptive Fe-Mn crusts are successfully removed by the leaching protocol. For example, the submarine samples with heavy, unleached values of ε^{205}Tl – including one submarine sample from the West Ka‘ena ridge that is noted to have visible Fe-Mn crusts – yield mantle values after being leached (Text S1). Furthermore, the Pb isotopic compositions of leached Hawaiian lavas, including in the samples used, are not as radiogenic as, nor trend towards, Pb from Pacific Fe-Mn crusts (e.g., Nobre Silva et al., 2009; Hanano et al., 2010; Harrison, 2017).

To assess the ε^{205}Tl values in the context of pre-established Hawaiian shield volcano geochemistry, samples are divided into three groups (Kea, Loa, and Enriched Loa) that have statistically different radiogenic isotopic compositions (Weis et al., 2020). These groups are named after the two geochemical Hawaiian trends (Kea and Loa) as well as the Ko‘olau volcano (subgroup of Loa, ‘Enriched Loa’), whose lavas define the isotopically enriched Hawaiian compositional end-member Enriched Makapu’u (‘EMK’; Tanaka et al., 2008). Performing a Student’s t-test on ε^{205}Tl values from Loa and Kea samples, including subaerial samples previously measured for ε^{205}Tl (Nielsen et al., 2006b), shows that these groups have statistically different means ($t(24) = 2.03$; $p = 0.05$; Table S1). Among the three Hawaiian geochemical groups, the median ε^{205}Tl is highest for the Kea group (-1.2, n = 18), followed by Loa (median is -1.6, n = 14), and Enriched Loa (median is -2.2, n = 6) (Figure 2b). When samples are further sub-divided into the statistically different geochemical subgroups identified in Weis et al. (2020), the median ε^{205}Tl is also different among subgroups (Figure 2b). The four samples with isotopically heavy Tl compositions are responsible for the overall larger range in Kea ε^{205}Tl values and three of them are outliers within the Kea geochemical group (Figure 2b). However, only two of these samples are outliers when further classified into their subgroups of Kea, Transitional Kea, and Kohala (Figure 2b). Of the trace elements analyzed, most incompatible elements show the differences between Loa-Kea volcanoes identified in previous studies (e.g., higher La/Th, La/Nb, and Sr/Nd in Loa lavas; Table S1; Salters et al., 2006; Pietruszka et al., 2013; Frey et al., 2016). However, three of the four samples with isotopically heavy ε^{205}Tl also have higher Cs, Ce, and incompatible trace elements including rare earth elements (discussed below).

The new data show a similar range in ε^{205}Tl values compared to previous Hawaiian data (i.e., Nielsen et al., 2006b) (Figure 2). However, the range in ε^{205}Tl from the previous study on Hawaiian lavas is primarily controlled by the values of three samples from Loa-trend volcanoes, whereas the range in our dataset is controlled by the values of samples from Kea-trend volcanoes (Figure 2a and 3a). One reason for the different range of ε^{205}Tl values between Loa and Kea volcanoes between studies may be the leaching procedure employed in this study as unleached submarine samples tend towards heavier ε^{205}Tl values (see Text S1).

4. Discussion

The overarching goal of this work was to investigate whether Hawaiian lavas have heterogeneous thallium isotopic compositions and determine if these compositions are the result of chemical heterogeneities in the Loa and Kea Hawaiian mantle sources. This study shows a small but resolvable difference in ε^{205}Tl between Hawaiian geochemical groups (Kea, Loa, Enriched Loa; Figure 2b). Unexpectedly, the Hawaiian samples that yielded a heavier and wider

range of ε^{205}Tl values are not from the Loa-trend volcanoes that sample isotopically enriched sources (in ^{208}Pb*/^{206}Pb* and ^{87}Sr/^{86}Sr), as previously found (Nielsen et al. 2006b), but are instead from the Kea-trend volcanoes (Figure 2).

When considering the ε^{205}Tl dataset as a whole, the mean ε^{205}Tl for all Hawaiian shield-stage basalts determined in this study is -1.3 ± 2.9 (2SD; median is -1.6). The range of ε^{205}Tl values measured in lavas from other OIB intraplate volcanic islands is significantly larger than found here (-6.4 to +6.6; Brett et al., 2021) and includes samples from Hawai‘i (Nielsen et al., 2006b), the Azores (Nielsen et al., 2007), Iceland (Nielsen et al., 2007; Prytulak et al., 2017), St. Helena (Blusztajn et al., 2018; Brett et al., 2021), Gough, Tristan da Cunha, Marquesas, and Austral-Cooks (Brett et al., 2021). Few statistically robust correlations between OIB ε^{205}Tl and radiogenic isotopes have been reported in the literature (e.g., Brett et al. 2021). However, our study offers a unique perspective, as the spatial resolution focuses on multiple volcanoes from a single volcanic island chain (Lō‘ihi to Kaua‘i;~550km and ~5 Ma). As such, the difference in ε^{205}Tl between Hawaiian geochemical groups (e.g., Figure 2b) may have important implications for the origin of heterogeneities in the mantle source of the Hawaiian volcanoes.

4.1 Sources of heavy ε^{205}Tl in Hawaiian leached lavas

Physical and chemical processes, such as degassing and post-eruptive alteration, can fractionate thallium isotopes – therefore, it is important to assess the potential influence of secondary processes on ε^{205}Tl before interpreting them as primary magmatic signatures. As such, the four leached Hawaiian samples with Tl isotopic compositions > 0 (Figure 2b) warrant further investigation. Foremost, other than being from the Kea geographic trend, the four heavy samples have few physical characteristics in common but do share a number of geochemical features: for example, these samples often have higher incompatible trace element concentrations and ratios (e.g., Th, Hf, V, Zn, U Cs/Tl, Ce/Tl, Ba/Rb, Rb/Tl, Pb/Tl, Nb/Y, Zr/Y, and REE in general; and Table S1). It is unlikely that this is due to smaller degrees of partial melting (i.e., if they were part of the more alkaline, transitional or post-shield phases of Hawaiian volcanism) because their Zr/Y and Nb/Y overlap with the wider sample set, confirming that they are shield-stage basalts (Figure S1b). Furthermore, the degree of partial melting should not fractionate Tl isotopes (e.g., Nielsen et al., 2017 and references therein).

Although it is difficult to unambiguously assess the effects of all secondary processes on ε^{205}Tl, some common approaches use certain trace elements and trace element ratios (e.g., Brett et al., 2021 and references therein). For example, Tl has a similar ionic radius and charge to K, Rb, and Cs and so these elements should behave similarly during mantle melting and crystallization (e.g., Nielsen et al., 2014; Nielsen et al., 2016; Nielsen et al., 2017b). Decoupling of these elements might indicate secondary processes: for example, the loss of volatile Tl through volcanic degassing or the addition/loss of mobile alkalic metals through post-eruptive alteration and fluid mobilization (e.g., Schiano et al., 1993; Nielsen et al., 2021). Below, we assess the possibility that degassing or alteration may have caused ε^{205}Tl >0 in the four samples from the Kea geochemical group (Figure 2b). The literature data discussed in this section are available in Tables S1 and S2.

4.1.1 Degassing

It has been debated whether volcanic degassing causes a measurable difference to ε^{205}Tl values because the net effect induced by kinetic fractionation during evaporation might be

balanced by condensation (Baker et al., 2009). However, recent work by Nielsen et al. (2021) shows that degassing can change the ε^{205}Tl of subaerial basalts: affected rocks show a positive correlation between ε^{205}Tl and Ce/Tl due to the preferential loss of the lighter ^{203}Tl isotope. Three of the four Hawaiian samples with isotopically heavy Tl have higher Ce/Tl than the other Hawaiian samples (Figure 3a): the highest Hawaiian values of Ce/Tl (2000 to 4500) are higher than upper mantle values (~1280; Nielsen et al., 2014), although are not as high as the values measured in one potentially degassed lava from Terceira, Azores (up to 17000; Nielsen et al., 2021). Importantly, of the seven samples with Ce/Tl > 2000, only three have heavy ε^{205}Tl: the other four have ε^{205}Tl < -0.7, including the samples with the highest Ce/Tl values measured (West Maui; 02-WA-10 and 00-LP-01; Figure 3a).

The analysis of multiple samples is required from a single volcano to determine whether degassing has affected their ε^{205}Tl values because this interpretation relies on the presence of a progressive increase in Ce/Tl with ε^{205}Tl in a related sample suite as the lighter ^{203}Tl is removed from the system (Nielsen et al., 2021). The samples from West Maui, which include two samples heavy in ε^{205}Tl, form the opposite trend, where Ce/Tl decreases as ε^{205}Tl increases (Figure 3a). A similar trend was noted in a study of samples from the Kilauea Iki lava lake, where samples with the lowest Tl concentrations had a range of ε^{205}Tl values and were not associated exclusively with heavy ε^{205}Tl (Gaschnig et al., 2021). If higher Ce/Tl values are indicative of degassing, this is either decoupled from Tl isotope systematics in Hawaiian shield lavas, or the samples with highest Ce/Tl are additionally altered with respect to Ce and/or Tl. The heavy ε^{205}Tl in two samples from a single eruption on Terceira, Azores are interpreted to result from degassing, although the authors stress that the majority of subaerial OIB lavas are likely unaffected by degassing (Nielsen et al., 2021).

In the case of Cs/Tl, the highest values measured in this study (~7) are from two of the four samples with heavy ε^{205}Tl; the other two heavy samples have lower Cs/Tl below the mantle value of ~6 (Nielsen et al., 2007) and are within the range of other Hawaiian samples (0.25-5; Figure 3b). When comparing Tl concentrations to those for Pb, samples from West Maui, west Kauaʻi, and Waiʻanae have higher Pb/Tl (Figure 3c). However, as is the case for many other trace elements, these samples also show a range of ε^{205}Tl that include both light and heavy values (Figure 3). The heavy sample from Hāna Ridge (K212-8; ε^{205}Tl = 2.0 ± 0.4) has the lowest Ce/Tl, Cs/Tl, and Pb/Tl of the entire sample set (135, 0.25, and 19, respectively; Figure 3). This sample either has slightly different source characteristics or was affected by different primary or secondary processes than the other Hawaiian samples with heavy values. Overall, given the observations noted above, degassing alone does not fully explain the anomalously heavy isotopic compositions of the Hawaiian samples from this study or the loss of Tl relative to elements such as Ce, Cs, Pb, and Rb (Figure 3).

There are other factors that can yield high Ce/Tl in OIB, including a lower sulphide to pyroxene ratio in the source (< 1500 ppm S) and overall heterogeneity of Ce/Tl in the mantle (Nielsen et al., 2014). With regards to the first factor, Tl concentrations between groundmass and groundmass sulphide crystals in Kīlauea Iki basalts were found to be heterogeneous, and fractionation of Tl towards heavier isotopic values from sulphide formation in the melt is estimated to require an average modal abundance of 6% sulphide blebs (Gaschnig et al., 2021). This modal abundance is not reached in the Kīlauea Iki samples given their low bulk S content (~700-1300 ppm; Gerlach and Graeber, 1985; Gaschnig et al., 2021). Although this is an

estimate for Kīlauea, it is likely representative of other Hawaiian tholeiites as Mauna Loa, Mauna Kea, Kīlauea, and Lōʻihi all have similar sulfur contents (Davis et al., 2003). The samples for which we have thin sections and hand samples do not have sulphide abundances close to the required estimate of Gaschnig et al. (2021) and as such it is unlikely that sulphide formation is the cause of the heavy Tl isotopic values.

Overall Ce/Tl heterogeneity in the mantle may explain Hawaiian Ce/Tl values, especially given that Hawaiian tholeiites often show trace element concentrations that vary between Loa and Kea geochemical groups (e.g., U, Th, etc.; Figure 4; Salters et al., 2006; Pietruszka et al., 2013; Frey et al., 2016). Cerium concentrations are negatively correlated with $^{208}Pb^*/^{206}Pb^*$, with Kea lavas generally having higher Ce and lower $^{208}Pb^*/^{206}Pb^*$ than the Loa lavas (Figure 4). A similar trend is observed for Ce/Tl vs. $^{208}Pb^*/^{206}Pb^*$ (Figure 4). These observations, as well as the elevated Ce/Tl associated with both heavy and light $\varepsilon^{205}Tl$ values (Figure 3a), favor a primary magmatic origin for elevated trace element concentrations and heavy $\varepsilon^{205}Tl$ values in the Hawaiian samples.

Finally, the West Maui samples have other isotopic characteristics that support a distinct or unique mantle source for their lavas: they have much lower $^{87}Sr/^{86}Sr$ for a given $^{206}Pb/^{208}Pb$ (Gaffney et al., 2004), and are part of a statistically unique geochemical group when compared to other Hawaiian volcanoes ("transitional Kea"; e.g., Figure 1b and inset of 2b; Weis et al., 2020). Explanations for these characteristics include assimilation of Pacific oceanic crust (Gaffney et al., 2004) and mantle heterogeneity sourced from the outside of the Pacific Large Low Shear Velocity Province (LLSVP) *via* the Hawaiian mantle plume (Weis et al., 2021); regardless, given that other studies suggest that the West Maui volcano consists of geochemically distinct Hawaiian shield lavas from a heterogeneous mantle source, it is plausible that this is also the case for the Ce/Tl and $\varepsilon^{205}Tl$ values measured in West Maui and other Kea volcanoes.

4.1.2 Alteration

Post-eruptive subaerial weathering may be linked to high Ce/Tl, as Tl can be mobilized during aqueous alteration, although it is unlikely that this process causes Tl isotope fractionation (Nielsen et al., 2005). The values of Th/Rb, Rb/Cs, and Ba/Rb in the Hawaiian samples (Figure 5) suggests that all five West Maui samples, as well as the west Kauaʻi (heavy) and Kohala (light) samples, may have experienced some Tl and (to a lesser extent) Rb loss (e.g., Nielsen et al., 2016; Nielsen et al., 2017). However, the highest Ce/Tl and Th/Rb values in this study (4541 and 0.37, respectively) are not nearly as high as previously measured values for altered Hawaiian lavas (~12000 and ~1.5; Nielsen et al., 2017b). When comparing Rb to Cs, there is no significant correlation with $\varepsilon^{205}Tl$ (Figure 5), and although most samples show higher Rb/Cs than the mantle value of ~75 (Nielsen et al., 2007), they are not high enough to indicate whether Rb or Cs were relatively gained or lost. Incompatible trace elements, such as Th and Ba (e.g., Nielsen et al., 2007), may provide additional insight on post-eruptive mobilization: Th/Tl vs. $\varepsilon^{205}Tl$ suggests Tl loss relative to Th for three of the four samples with heavy $\varepsilon^{205}Tl$ values (Figure 5); however, once again, the two samples with highest Th/Tl ratios are not heavy in $\varepsilon^{205}Tl$ and the Hāna Ridge sample does not show a similar relationship. The Ba/Rb is similarly ambiguous when compared to $\varepsilon^{205}Tl$, as a number of samples have higher Ba/Rb but their corresponding $\varepsilon^{205}Tl$ value is not necessarily heavy (Figure 5).

Although subaerial alteration minerals should be removed by the leaching protocol, given the ambiguity of trace element ratios presented, we cannot discount the possibility that a small

percentage were incompletely removed (e.g., Hanano et al., 2009). Secondary minerals are common in Hawaiian basalts and typically include hydrothermal alteration products such as clays (e.g., smectite), zeolites (e.g., chabazite and phillipsite), Fe-rich goethite, and rarely, pyrite (Hanano et al., 2009 and references therein).The West Maui samples with heavy ε^{205}Tl (01-MA-560 and 01-MA-1020) are core samples (the other three isotopically light samples were collected subaerially) and are described in the literature as having visible oxidation and Fe-staining (Gaffney et al., 2004). Hypothetically, as these samples were originally buried within the volcanic edifice, it could be possible that they were subjected to moderate- to high-temperature metasomatism by circulating fluids that were capable of mobilizing isotopically heavy Tl scavenged from hydrothermal Mn deposits or hydrogenetic Fe-Mn crusts (e.g., Rehkämper et al., 2002). However, this scenario is hypothetical and would need to be tested.

4.1.4 Summary

The geochemical indicators of Tl fractionation from degassing, sulphide formation, or alteration do not vary systematically in the samples from this study, nor do they always occur in conjunction with isotopically heavy ε^{205}Tl values. On a sample-by-sample basis, evidence for degassing or post-eruptive alteration in the two West Maui samples is ambiguous (e.g., opposite Ce/Tl vs. ε^{205}Tl trend); however, this does not exclude the possibility that both degassing and alteration may have occurred, and the concurrence of these processes disturbed the primary Tl isotopic signature. The sample from west Kaua‘i that is isotopically heavy has geochemical characteristics similar to the two West Maui samples that also have heavy ε^{205}Tl, and so may be the result of a similar combination of physical and/or chemical mechanisms. In the case of the Hāna Ridge sample that has heavy values, it has the highest Tl concentration measured (263 ng/g) and a positive ε^{205}Tl value (2.0 ± 0.2); for this sample, we are confident that its ε^{205}Tl value is primary. Overall, we have no systematic evidence for the influence of degassing or secondary, post-eruptive processes on the Tl isotopic composition of leached lavas in this study, however, we emphasize that future studies of ε^{205}Tl in OIB should include multiple samples from single volcanoes to more robustly assess degassing effects (Nielsen et al., 2021).

4.2 Origin of Tl isotopic heterogeneity in Hawaiian shield basalt

Hawaiian basalts, and OIB in general, have heterogeneous radiogenic isotopic compositions that indicate the presence of chemical heterogeneities in their sources (e.g., Weis et al., 2011; White 2015). When compared to radiogenic isotopes for the same samples (Tables S1 and S2), the ε^{205}Tl data from this study do not form statistically meaningful trends (Figure 6), which is consistent with previous findings for OIB (Brett et al., 2021). However, these comparisons further demonstrate the varying ranges of ε^{205}Tl between each geochemical group (Loa, Kea, Enriched Loa) (e.g., Figure 6). The Loa group samples are much more homogeneous with respect to ε^{205}Tl than both the Kea and Enriched Loa groups (Figure 6). The previously identified trends between ε^{205}Tl and ^{206}Pb/^{204}Pb and ^{208}Pb/^{204}Pb for samples from Loa volcanoes (Nielsen et al., 2006b) are not as evident in the new dataset (e.g., Figure in Text S1). Differences between this study and that of Nielsen et al. (2006b) include the number of samples used, number of volcanoes represented, sample rock type (mainly basalt in this study *vs.* picritic basalt in Nielsen et al. (2006b) – although, samples from this study have a wide range of MgO wt%), and the leaching procedure used in this study to remove secondary alteration (Text S1). The leaching protocol may account for some of the differences in Hawaiian ε^{205}Tl values and trends observed in the submarine Loa samples from Nielsen et al. (2006b) *versus* those from this study. Acid leaching is a necessary step for removing erroneous isotopic compositions induced by

secondary processes (e.g., Nobre Silva et al., 2009; Hanano et al., 2009) and also for obtaining the primary Tl isotopic composition of the rocks (Nielsen et al., 2016). This is consistent with results from other OIB isotopic studies (e.g., Harrison et al., 2017; Nobre Silva et al., 2013) and is mainly important for submarine samples, as these are more likely to contain post-eruptive Fe-Mn crusts with heavy ε^{205}Tl values (e.g., Nielsen et al., 2016). However, it is possible that the heavy values previously obtained in Hawaiian samples (i.e., Nielsen et al., 2006b), even if from submarine samples potentially contaminated by accumulated Fe-Mn crusts, are primary mantle signatures that reflect source heterogeneity.

Isotopically heavy values of ε^{205}Tl in OIB have previously been attributed to the presence of either ancient ferromanganese or pelagic sediment recycled through the mantle (e.g., Nielsen et al., 2006b; Brett et al., 2021), modern ferromanganese or pelagic sediment assimilated during magma ascent (e.g., Nielsen et al., 2007; Brett et al., 2021), or fractionation from volcanic degassing (Nielsen et al., 2021). The extreme Tl concentration contrast between the mantle (<1 ng/g) and potential surface inputs (>>100 ng/g) can disturb Tl isotopic systematics without resolvable effect on other geochemical signatures (radiogenic isotopes, trace elements) (e.g., Blusztajn et al., 2018). This effect can lead to challenges in determining whether sediment-derived Tl is acquired in the mantle source or from the crust during magma ascent (Brett et al., 2021). Nonetheless, the statistical difference in ε^{205}Tl between the Loa and Kea geochemical groups (e.g., Figure 2) is difficult to reconcile with either degassing or modern sediment assimilated before eruption as these processes would have to dominantly occur along only one side of the volcanic chain, i.e., only for Kea-trend volcanoes and the Makapu‘u section of Ko‘olau volcano (Enriched Loa) given the range in ε^{205}Tl values for this group when including previous data from Nielsen et al. (2006b) (Figure 6). The Hf-Nd systematics of Enriched Loa lavas have been attributed to the influence of recycled pelagic sediment in the enriched Hawaiian source (e.g., Blichert-Toft et al., 1999). Ko‘olau lavas are the main group of lavas that define the Enriched Loa geochemical end-member and are distinct in most radiogenic isotopic compositions and trace element concentrations from other Hawaiian lavas (e.g., Figures 4 and 6). The fact that they show a range in ε^{205}Tl values is not surprising. In addition, previous work has shown that the Pb isotopic compositions of leached Hawaiian lavas are not as radiogenic as those from modern Pacific ferromanganese crusts (e.g., Nobre Silva et al., 2009; Hanano et al., 2010), which supports a recycled mantle origin for the ε^{205}Tl systematics observed as previously suggested by Nielsen et al. (2006b).

As a first-order, reconnaissance-type approach to gain further insight on the origin of the wide range of ε^{205}Tl values measured, we compiled data for shield-stage Hawaiian lavas from two other isotopic systems that are used as indicators of recycled surface materials (δ^{18}O and ^{138}Ce/^{142}Ce; total n = 138 and 8). Data from ^{3}He/^{4}He$_{(R/RA)}$ and μ^{182}W isotopes were also compiled (total n = 455 and 12) to explore whether ε^{205}Tl shows relationships with isotopic indicators of undegassed (e.g., primordial) or primitive sources, respectively. Isotopic means for each volcano were calculated because individual samples rarely have data available for more than one isotopic system. The data and data sources are available in supporting information Table S3.

When compared to the compiled dataset, Kea-group volcanoes show a potential weak increase in ε^{205}Tl with increasing δ^{18}O (Figure 7a) and ^{3}He/^{4}He$_{(R/RA)}$ values (Figure S2) and no statistically meaningful trends with ^{138}Ce/^{142}Ce and μ^{182}W (Figure S2). The Loa and Enriched

Loa volcanoes show a range of values for the O, Ce, He, and W isotopes, but no clear trends are observed when compared to ε^{205}Tl (Figure 7a and Figure S2). The Kea samples with highest δ^{18}O are part of a new geochemical subgroup recently identified within the Kea group using a statistical approach on a large (n > ~600) database of high-precision radiogenic isotopic analyses (Figure 7b) ('Kohala' subgroup; Weis et al., 2020). Additional O isotopic analyses on samples from the 'transitional Kea' geochemical subgroup (see Weis et al., 2020) might yield higher δ^{18}O values than the Kohala subgroup alone, similar to ε^{205}Tl (Figure 7b). Higher δ^{18}O values for Kea volcanoes associated with heavier ε^{205}Tl values (Figure 7) could be the result of a recycled origin for any Tl-heavy surface material incorporated in the higher-ε^{205}Tl Kea volcanoes because assimilation of shallow crustal rocks (having interacted with high-temperature meteoric waters) and seawater, both presumably incorporated along with any modern ferromanganese crusts or sediment, should lower the δ^{18}O values in resulting lavas (Bindeman, 2008). The inherently low δ^{18}O values in Kea volcano shield lavas relative to other OIB could be a feature of the Kea mantle end-member (e.g., Eiler et al., 1996; Eiler 2001).

Higher ^{138}Ce/^{142}Ce in OIB has been attributed to old (potentially pre-Great Oxygenation Event (GOE)), recycled oceanic sediments (Israel et al., 2020). However, there are not enough Ce isotopic data for Hawaiian shield basalts from all three main geochemical groups (Loa, Kea, and Enriched Loa) to make robust comparisons to Tl (Figure S2). Previously, Ce/Ce* anomalies <1 (Ce concentration relative to primitive mantle) were attributed to the presence of recycled oceanic sediments in Gough Island lavas (Class and le Roex, 2008). However, Israel et al. (2020) found that the compositions of enriched, EM-affinity lavas can be reproduced using recycled oceanic sediment that does not have negative Ce anomalies. Although the Kea lavas are not EM-like, this demonstrates that heavy ε^{205}Tl values resulting from recycled oceanic sediment would not require a Ce anomaly, which is what is observed for the Kea lavas with heavier ε^{205}Tl (Figure S2). Additional analyses of Ce isotopes on a range of Hawaiian lavas would potentially provide further information on the nature and age of recycled sediments in the Kea source – for example, whether these sediments were recycled into the mantle pre- or post-GOE (i.e., Israel et al., 2020).

The above observations are preliminary and require further testing. However, the fact that certain Loa and Kea volcanoes both show elevated δ^{18}O, but different ε^{205}Tl, Pb, and Sr isotopic compositions, could provide important information about the nature of the recycled surface materials contributing to their isotopic heterogeneity: certain isotopic systems (e.g., δ^{18}O) may indicate the presence of recycled surface materials in the deep mantle source, but cannot discriminate between the type of material, whereas other isotopic or trace element systems (e.g., ε^{205}Tl and even Ce/Ce*) may be able to. For certain Kea volcanoes (e.g., West Maui/'Transitional Kea' (Figure 2b); Weis et al., 2020), a pelagic or oceanic sediment coupled to slab debris (e.g., oceanic crust) could account for the higher ε^{205}Tl (this study), δ^{18}O (e.g., Woodhead et al., 1993; Harmon and Hoefs 1995; Eiler et al., 1996; Bindeman 2008 and references therein), and ^{143}Nd/^{144}Nd and ^{176}Hf/^{177}Hf (e.g., Blichert-Toft et al., 1999; Chauvel et al., 2008, Carpentier et al., 2014). Conversely, the radiogenic isotopic ratios of Loa and Enriched Loa volcanoes (i.e., Mauna Loa, Ko'olau) that trend toward EM-1 mantle compositions could be accounted for by the presence of tectonically eroded and subducted lower continental crust and/or sediment, producing mantle-like ε^{205}Tl and higher δ^{18}O, ^{208}Pb*/^{206}Pb*, and ^{87}Sr/^{86}Sr compositions (higher source Th/U and Rb for the latter two isotopic systems). The heavier ε^{205}Tl present in both Ko'olau and Kea lavas, coupled with very different Hf-Nd systematics (e.g.,

Blichert-Toft et al., 1999) and low and high $^{206}Pb/^{204}Pb$, respectively (e.g., Figure 1b; Weis et al., 2020), may reflect the incorporation of different types of crust and sediment in their respective mantle sources. Thus, this study suggests that surface-derived materials recycled into the mantle are conceivably present in both the Loa and Kea deep mantle sources, but have different origins and recycling histories, and potentially different ages. This is not out of the realm of possibility as multiple studies now suggest that the lower mantle near the CMB is likely heterogeneous and may contain multiple, isotopically distinct chemical reservoirs (e.g., Starkey et al., 2016; Torsvik et al., 2016; Parai et al., 2019; Harpp and Weis, 2020; Mundl-Petermeier et al., 2020; Weis et al., 2020). Overall, additional multi-isotopic work (including the noble gases, e.g., Xe and Ne; Parai et al., 2019) on the same samples is needed to substantiate the above observations and to better constrain the composition, sources, and age of these recycled materials. However, the comparisons made in this study demonstrate that interesting trends between traditional and non-traditional stable isotopes in Hawaiian shield lavas can be delineated with high density sampling and corroborates the approach of other recent work that combines novel and traditional isotopic systems (e.g., see also Starkey et al., 2016; Israel et al., 2020; Mundl-Petermeier et al., 2020; etc.).

4.3 Implications for the Kea Hawaiian source(s) and deep Pacific mantle

The Loa and Kea geochemical and geographic trends observed on the islands of Hawai‘i to Moloka‘i (Figure 1; e.g., Abouchami et al., 2005) are thought to represent two compositional domains in the Hawaiian plume, with a boundary trending roughly northwest-southeast (Figure 1, inset), that are hypothesized to extend to the base of the plume near the CMB (e.g., Abouchami et al., 2005; Hofmann and Farnetani, 2013; Hanano et al., 2010; Weis et al., 2011; French and Romanowicz 2015; Williamson et al., 2019; Weis et al., 2020). In this model, the northeastern domain of the plume supplies the Kea-trend volcanoes from an ‘ambient Pacific mantle’ source on the outside of the Pacific LLSVP (e.g., Weis et al., 2011; Harrison et al., 2017; Weis et al., 2020), whereas the southwestern domain supplies the Loa-trend volcanoes from a source within the Pacific LLSVP (Weis et al., 2011; Harrison et al., 2017) that contains recycled surface and/or primordial material (e.g., Torsvik et al., 2016; Mundl-Petermeier et al., 2020). The ‘Enriched Loa’ volcanoes (Makapu‘u [Ko‘olau] and Lāna‘i) sample additional heterogeneities from within the Loa domain that are hypothesized to be sourced from the ULVZ within the LLSVP (Weis et al., 2011; Harrison et al., 2017; Weis et al., 2020).

If $\varepsilon^{205}Tl > 0$ in Hawaiian lavas is the result of recycled surface materials in the Hawaiian source, this material is dominantly being sampled on the Kea (northeast) side of the plume (Figure 1). This outcome is the opposite of what is expected given that typically, the Loa and Enriched Loa group of volcanoes show geochemical indicators (isotope and trace element systematics) of recycled surface materials in their source (e.g., Abouchami et al., 2005; Huang and Frey, 2005; Fekiacova et al., 2007; Tanaka et al., 2008; Weis et al., 2011; Jackson et al., 2012). This study =supports recent work (i.e., Weis et al., 2020) that shows that the Kea-trend geochemical group is compositionally heterogeneous and can be further divided into distinct geochemical subgroups. The Kea samples from this study have more heterogenous $\varepsilon^{205}Tl$ values than the Loa samples, and the ‘Transitional Kea’ subgroup, which is statistically distinct in radiogenic isotopes (Weis et al., 2020), is also different in $\varepsilon^{205}Tl$ (e.g., Figure 2 and 5). Thus, like the Loa volcanoes, the deep mantle source of Kea volcanoes is likely chemically heterogeneous but on more compositionally restricted scale (e.g., Weis et al., 2011) and with different materials contributing the heterogeneities. Projecting to the CMB, geophysical studies have imaged

subducted slab debris adjacent to the outer edge of the LLSVP beneath Hawai‘i (e.g., Sun et al., 2019). Assuming a compositionally bilateral mantle plume, we propose that Kea-trend volcanoes sample both ambient Pacific mantle (‘PREMA’) as well as subducted slab-related heterogeneities (e.g., pelagic sediments), as long as the sediments and their corresponding oceanic crust remain coupled (e.g., Chauvel et al., 2008) or are both present individually. The presence of slab debris, associated sediments, and potentially primordial material located on the outside of the Pacific LLSVP (e.g., Torsvik et al., 2016; Weis et al., 2020) is plausible and has been modelled geophysically (e.g., Dannberg and Gassmöller, 2018; Sun et al., 2019) and geochemically (e.g., Parai et al., 2019; Mundl-Petermeier et al., 2020). The implication is that the deep, ‘ambient’ mantle on the Kea side of the Hawaiian plume and on the outside of the Pacific LLSVP is heterogeneous and includes a variety of chemical reservoirs, including PREMA (White 2015 and references therein), oceanic crust and sediments (e.g., Chauvel et al., 2008; Torsvik et al., 2016), as well as variably undegassed and primitive materials (e.g., Williams et al., 2015; Mundl-Petermeier et al., 2020; Text S3).

5. Conclusions

Thallium isotopic compositions were measured in 34 acid-leached samples of shield-stage basalt from 13 volcanoes that span the entire geographic and geochemical range of the Hawaiian Islands, from Lō‘ihi to Kaua‘i. High-density sampling, rigorous sample pre-treatment, and careful assessment of ε^{205}Tl values on a sample-by-sample basis that takes into account geography, rock type, sample context (subaerial, submarine), alteration, as well as major element, trace element, and other isotopic data, has allowed us to document ε^{205}Tl differences between Hawaiian geochemical groups (Kea, Loa, Enriched Loa) and subgroups (Transitional Kea, Kohala, Kea, Average Loa, Lō‘ihi, Enriched Loa). In particular, Kea-trend volcanoes show heavier primary magmatic ε^{205}Tl values that potentially correspond with higher δ^{18}O values. The leaching procedure used and exclusion of secondary trace element signatures suggests that the ε^{205}Tl variations are primary and were acquired from the mantle source of the lavas. Thus, surface materials such as ferromanganese-rich pelagic sediment recycled into the mantle may provide chemical heterogeneities on the Kea side of the Hawaiian plume. Results from this study suggest the presence of recycled materials in both the Loa and Kea Hawaiian sources and support a heterogeneous lower mantle within the Pacific LLSVP, to the southwest of Hawai‘i, as well as on the outside of the Pacific LLSVP, to the northeast of Hawai‘i in the deep Pacific mantle.

Acknowledgements

Our thanks go to Dr. Aaron Pietruszka for providing samples from Kīlauea, Drs. Amy Gaffney and Bruce Nelson for providing samples from West Mau‘i, and JAMSTEC for providing samples from the Hāna Ridge. Sincere thanks go to Kathy Gordon and Dr. Marg Amini for their support and guidance while setting up the analytical procedure at PCIGR and Vivian Lai for her support with trace element analyses. Thank you to Drs. Jamie Cutts and Alice Chang for very helpful edits. We are thankful to Dr. Janne Blichert-Toft for her editorial handling and to Drs. Sune Nielsen, Bill White, and Mathias Schannor for their constructive reviews. Funding for this work was provided by an NSERC Discovery Grant to Dr. D. Weis. JP and DW acknowledge the International Research Opportunities Program (IROP) exchange between Imperial College London and the University of British Columbia, which enabled the initial thallium isotope collaboration.

Data Availability Statement

All data collected during this study, as well as published data used in figures and text, can be found in the supporting information tables (Tables S1, S2, and S3), which are available for download from the publicly accessible Scholars Portal Dataverse (insert doi link here when link is provided).

References

Abouchami, W., Galer, S. J. G., & Hofmann, A. W. (2000). High precision lead isotope systematics of lavas from the Hawaiian scientific drilling project. Chemical Geology, 169(1–2), 187–209. https://doi.org/10.1016/s0009-2541(00)00328-4

Abouchami, W., Hofmann, A. W., Galer, S. J. G., Frey, F. A., Eisele, J., & Feigenson, M. (2005). Lead isotopes reveal bilateral asymmetry and vertical continuity in the Hawaiian mantle plume. Nature, 434(7035), 851–856. https://doi.org/10.1038/nature03402

Baker, R.G.A., Rehkämper, M., Hinkley, T.K., Nielsen, S.G., & Toutain, J.P. (2009). Investigation of thallium fluxes from subaerial volcanism—implications for the present and past mass balance of thallium in the oceans. Geochimica et Cosmochimica Acta, 73(20), 6340-6359.

Bindeman, I. (2008). Oxygen isotopes in mantle and crustal magmas as revealed by single crystal analysis. Reviews in Mineralogy & Geochemistry, 69, 445-478. doi: 10.2138/rmg.2008.69.12

Blichert-Toft J., Frey, F.A., Albarède, F.(1999) Hf Isotope Evidence for Pelagic Sediments in the Source of Hawaiian Basalts. Science, 285, 879-882.

Blusztajn J., Nielsen S. G., Marschall H. R., Shu Y., Ostrander C. M. and Hanyu T. (2018). Thallium isotope systematics in volcanic rocks from St Helena - constraints on the origin of the HIMU reservoir. Chem. Geol. 476 , 292–301. doi:10.1016/j.chemgeo.2017.11.025

Bower, D.J., Gurnis, M., Seton, M. (2013) Lower mantle structure from paleogeographically constrained dynamic Earth models. Geochem. Geophys. Geosyst., 14 (1), 44-63.

Brett, A., Prytulak, J., Hammond, S.J., Rehkämper, M. (2018). Thallium Mass Fraction and Stable Isotope Ratios of Sixteen Geological Reference Materials. Geostandards and Geoanalytical Research, 42, 339-360.

Brett, A., Prytulak, J., Rehkämper, M., Hammond, S.J., Chauvel, C., Stracke, A., Willbold, M. (2021) Thallium elemental and isotopic systematics in ocean island lavas. Geochimica et Cosmochimica Acta, 301, 187-210.

Carpentier M., D. Weis, Chauvel, C. (2013). Large U loss during weathering of upper continental crust: The sedimentary record, Chem. Geol., 340, 91–104, doi:10.1016/j.chemgeo.2012.12.016

Carpentier, M., Weis, D., Chauvel, C. (2014). Fractionation of Sr and Hf isotopes by mineral sorting in Cascadia Basin terrigenous sediments. Chemical Geology, 382, 67-82.

Chauvel, C., Lewin, E., Carpentier, M., Arndt, N.T., Marini, J-C. (2008). Role of recycled oceanic basalt and sediment in generating the Hf-Nd mantle array. Nature Geoscience 1, 64-67. doi: 10.1038/ngeo.2007.51

Class, C. and le Roex, A.P. (2008). Ce anomalies in Gough Island lavas — Trace element characteristics of a recycled sediment component. Earth and Planetary Science Letters, 265, 475-486.

Craig, J.D., Andrews, J.E., Meylan, M.A., (1982). Ferromanganese deposits in the Hawaiian Archipalago. Marine Geology, 45, 127-157.

Dannberg, J., Gassmöller, R. (2018). Chemical trends in ocean islands explained by plume–slab interaction. Proceedings of the National Academy of Sciences 115(17), 4351-4356.

Davis, M.G., Garcia, M.O., Wallace, P. (2003). Volatiles in glasses from Mauna Loa Volcano, Hawai'i: implications for magma degassing and contamination, and growth of Hawaiian volcanoes. Contrib Mineral Petrol, 144, 570–591, DOI 10.1007/s00410-002-0416-z

DePaolo, D. J., Bryce, J. G., Dodson, A., Shuster, D. L., & Kennedy, B. M. (2001). Isotopic evolution of Mauna Loa and the chemical structure of the Hawaiian plume. Geochemistry, Geophysics, Geosystems, 2(7). https://doi.org/10.1029/2000GC000139

Eggins, S.M., Woodhead, J.D., Kinsley, L.P.J, Mortimer, G.E., Sylvester, P., McCulloch, M.T., Hergt, J.M., Handler, M.R. (1997). A simple method for the precise determination of > 40 trace elements in geological samples by ICPMS using enriched isotope internal standardization. Chemical Geology, 134, 311-326.

Eiler, J.M. (2001). Oxygen isotope variations of basaltic lavas and upper mantle rocks. In: Valley, J. W. & Cole, D. R. (eds) Stable Isotope Geochemistry. Mineralogical Society of America, Reviews in Mineralogy 43, 319-364.

Eiler, J.M., Farley, K.A.,Valley, J.W., Hofmann, A., Stolper, E.M. (1996). Oxygen isotope constraints on the sources of Hawaiian volcanism. Earth and Planetary Science Letters 144, 453-468.

Eisele, J., Abouchami, W., Galer, S.J.G., Hofmann, A.W. (2003). The 320 kyr Pb isotope evolution of Mauna Kea lavas recorded in the HSDP-2 drill core. Geochem. Geophys. Geosyst. 4(5), 8710.

Fekiacova, Z., Abouchami, W., Galer, S.J.G., Garcia, M.O., Hofmann, A.W. (2007). Origin and temporal evolution of Koʻolau Volcano, Hawaiʻi: Inferences from isotope data on the Koʻolau scientific drilling project (KSDP), the Honolulu volcanics and ODP Site 843. Earth Planet. Sci. Lett. 261, 65-83.

768 Fitzpayne A., Prytulak J., Giuliani A. and Hergt J. (2020) Thallium isotopic composition of
769 phlogopite in kimberlite-hosted MARID and PIC mantle xenoliths. Chemical Geololgy, 531
770 119347.
771
772 Fourny, A., Weis, D., & Scoates, J.S. (2016). Comprehensive Pb-Sr-Nd-Hf isotopic, trace
773 element, and mineralogical characterization of mafic to ultramafic rock reference materials.
774 Geochemistry, Geophysics, Geosystems, 17(3), 739-773.
775
776 French, S.W. and Romanowicz, B. (2015). Broad plumes rooted at the base of the Earth's mantle
777 beneath major hotspots. Nature 525, 95-99.
778
779 Frey, F.A., Garcia, M.O., Roden, M.F. (1994). Geochemical characteristics of Koolau Volcano:
780 Implications of intershield geochemical differences among Hawaiian volcanoes. Geochimica et
781 Cosmochimica Acta, 58, 1441-1462.
782
783 Frey, F.A., Huang, S., Xu, G., Jochum, K.P. (2016). The geochemical components that
784 distinguish Loa- and Kea-trend Hawaiian shield lavas. Geochimica et Cosmochimica Acta, 185,
785 160-181.
786
787 Gaffney, A.M., Nelson, B.K., Blitchert-Toft, J. (2004). Geochemical Constraints on the Role of
788 Oceanic Lithosphere in Intra-Volcano Heterogeneity at West Maui, Hawaii. Journal of
789 Petrology, 45 (8), 1663-1687
790
791 Galer, S. J. G., & Abouchami, W. (1998). Practical application of lead triple spiking for
792 correction of instrumental mass discrimination. Mineralogical Magazine, 62A, 491–492.
793
794 Gaschnig, R.M, Rader, S.T., Reinhard, C.T., Owens, J.D., Planavsky, N., Wang, X., Asael, D.,
795 Greaney, A., Helz, R. (2021). Behavior of the Mo, Tl, and U isotope systems during
796 differentiation in the Kilauea Iki lava lake. Chemical Geology, 574,
797 doi.org/10.1016/j.chemgeo.2021.120239
798
799 Gerlach, T.M., Graeber, E.J. (1985). Volatile budget of Kilauea volcano. Nature, 313, 273-276.
800
801 Govindaraju, K. (1994). 1994 Compilation of Working Values and Descriptions for 383
802 Geostandards, Geostandards Newsletter, 18, 1-158.
803
804 Greene, A.R., Garcia, M.O., Pietruszka, A.J., Weis, D., Marske, J.P., Vollinger, M.J., & Eiler, J.
805 (2013). Temporal geochemical variations in lavas from Kilauea's Puu Oo eruption (1983–2010):
806 Cyclic variations from melting of source heterogeneities. Geochemistry, Geophysics,
807 Geosystems, 14, 4849–4873, doi: 10.1002/ggge.20285
808
809 Hanano, D., Scoates, J. S., & Weis, D. (2009). Alteration mineralogy and the effect of acid
810 leaching on the Pb-isotope systematics of ocean island basalts. American Mineralogist, 94(1),
811 17–26. https://doi.org/10.2138/am.2009.2845
812

Hanano, D., Weis, D., Scoates, J. S., Aciego, S., & DePaolo, D. J. (2010). Horizontal and vertical zoning of heterogeneities in the Hawaiian mantle plume from the geochemistry of consecutive postshield volcano pairs: Kohala-Mahukona and Mauna Kea-Hualalai. Geochemistry, Geophysics, Geosystems, 11, Q01004. https://doi.org/10.1029/2009GC002782

Harmon, R.S and Hoefs, J. (1995). Oxygen isotope heterogeneity of the mantle deduced from global ^{18}O systematics of basalts from different geotectonic settings. Contrib. Mineral. Petrol. 120, 95-114.

Harpp, K.S., Weis, D. (2020). Insights into the Origins and Compositions of Mantle Plumes: A Comparison of Galápagos and Hawai'i. Geochem. Geophys. Geosyst. 21(9), e2019GC00888

Harrison, L.N., Weis, D., Hanano, D., Barnes E. (2015). Lithium Isotopic Signature of Hawaiian Basalts, In Carey, R., Cayol, V., Poland, M., & Weis, D. (Eds.), Hawaiian Volcanoes: From Source to Surface, Geophysical Monograph 208, 79-104

Harrison, L.N. (2017) Isotopic and chemical heterogeneity of the Hawaiian mantle plume: Evaluating mantle geodynamics and characterization of the Loa geochemical trend. PhD thesis, University of British Columbia

Harrison, L. N., Weis, D., & Garcia, M. O. (2017). The link between Hawaiian mantle plume composition, magmatic flux, and deep mantle geodynamics. Earth and Planetary Science Letters, 463, 298–309. https://doi.org/10.1016/j.epsl.2017.01.027

Harrison, L. N., & Weis, D. (2018). The size and emergence of geochemical heterogeneities in the Hawaiian mantle plume constrained by Sr-Nd-Hf isotopic variation over ~47 million years. Geochemistry, Geophysics, Geosystems, 19, 2823–2842. https://doi.org/10.1029/2017GC007389

Hein, J.R. and Koschinsky, A. (2014). Deep-ocean ferromanganese crusts and nodules. Treatise on Geochemistry (2nd edition), 13, 273-291.

Hofmann, A. W. (2014). Sampling mantle heterogeneity through oceanic basalts: Isotopes and trace elements. In R. W. Carlson, H. D. Holland, & K. K. Turekian (Eds.), Treatise on Geochemistry, (Second ed., Vol. 3, pp. 67–101). Amsterdam: Elsevier. https://doi.org/10.1016/B978-0-08-095975-7.00203-5

Hofmann, A.W., Farnetani, C.G., 2013. Two views of Hawaiian plume structure. Geochem. Geophys. Geosys. 14, 5308–5322. https://doi.org/10.1002/2013GC00494

Hofmann, A.W. and White, W.M. (1982). Mantle plumes from ancient oceanic crust. Earth and Planetary Science Letters, 57, 421-436.

Huang, S. and Frey, F.A. (2005). Recycled oceanic crust in the Hawaiian Plume: evidence from temporal geochemical variations within the Koolau Shield. Contrib. Mineral. Petrol., 149, 556-575.

Israel, C., Boyet, M., Doucelance, R., Bonnand, P., Frossard, P., Auclair, D., Bouvier, A. (2020). Formation of the Ce-Nd mantle array: Crustal extraction vs. recycling by subduction. Earth and Planetary Science Letters, 530, doi: 10.1016/j.epsl.2019.115941

Jackson, E. D., Silver, E. A., & Dalrymple, G. B. (1972). Hawaiian-emperor chain and its relation to Cenozoic circumpacific tectonics. Bulletin Geological Society of America, 83(3), 601–618. https://doi.org/10.1130/0016-7606(1972)83[601:HCAIRT]2.0.CO;2

Jackson, M. G., Weis, D., & Huang, S. (2012). Major element variations in Hawaiian shield lavas: Source features and perspectives from global ocean island basalt (OIB) systematics. Geochemistry, Geophysics, Geosystems, 13, Q09009. https://doi.org/10.1029/2012GC004268

Li, M., McNamara, A.K., Garnero, E.J., Yu, S. (2017). Compositionally-distinct ultra-low velocity zones on Earth's core-mantle boundary. Nat. Comm. 8, 177.

McNamara, A.K., Garnero, E.J., Rost, S. (2010). Tracking deep mantle reservoirs with ultra-low velocity zones. Earth Planet. Sci. Lett. 299, 1-9.

Montelli, R., Nolet, G., Dahlen, F. A., & Masters, G. (2006). A catalogue of deep mantle plumes: New results from finite frequency tomography. Geochemistry, Geophysics, Geosystems, 7, Q11007. https://doi.org/10.1029/2006GC001248

Mundl-Petermeier, A., Walker, R.J., Fischer, R.A., Lekic, V., Jackson, M.G., Kurz, M.D. (2020). Anomalous ^{182}W in high $^{3}He/^{4}He$ ocean island basalts: Fingerprints of Earth's core? Geochimica et Cosmochimica Acta, 271, 194-211. doi: 10.1016/j.gca.2019.12.020

Nielsen, S. G., Rehkämper, M., Porcelli, D., Andersson, P., Halliday, A. N., Swarzenski, P. W., ... & Günther, D. (2005). Thallium isotope composition of the upper continental crust and rivers—an investigation of the continental sources of dissolved marine thallium. Geochimica et Cosmochimica Acta, 69(8), 2007-2019.

Nielsen, S.G., Rehkämper, M., Teagle, D.A., Butterfield, D.A., Alt, J.C., & Halliday, A.N. (2006a). Hydrothermal fluid fluxes calculated from the isotopic mass balance of thallium in the ocean crust. Earth and Planetary Science Letters, 251(1), 120-133.

Nielsen, S.G., Rehkämper, M., Norman, M.D., Halliday, A.N., & Harrison, D. (2006b). Thallium isotopic evidence for ferromanganese sediments in the mantle source of Hawaiian basalts. Nature, 439(7074), 314-317.

Nielsen, S.G., Rehkämper, M., Brandon, A.D., Norman, M.D., Turner, S., & O'Reilly, S.Y. (2007). Thallium isotopes in Iceland and Azores lavas—implications for the role of altered crust and mantle geochemistry. Earth and Planetary Science Letters, 264(1), 332-345.

Nielsen, S. G., Wasylenki, L. E., Rehkämper, M., Peacock, C. L., Xue, Z., Moon, E. M. (2013). Towards an understanding of thallium isotope fractionation during adsorption to manganese oxides, Geochim. Cosmochim. Acta, 117, 252–265.

Nielsen, S.G., Shimizu, N., Lee, C.T.A., Behn, M. (2014). Chalcophile behavior of thallium during MORB melting and implications for the sulfur content of the mantle. Geochemistry, Geophysics, Geosystems, 15, 4905-4919

Nielsen, S.G., Klein, F., Kading, T., Blusztajn, J., Wickham, K (2015). Thallium as a tracer of fluid-rock interaction in the shallow Mariana forearc. Earth and Planetary Science Letters, 430, 416-426.

Nielsen, S.G., Yogodzinski, G., Prytulak, J., Plank, T., Kay, S.M., Kay, R.W., ... & Kading, T. (2016). Tracking along-arc sediment inputs to the Aleutian arc using thallium isotopes. Geochimica et Cosmochimica Acta, 181, 217-237.

Nielsen, S.G., Rehkämper, M., & Prytulak, J. (2017a). Investigation and application of thallium isotope fractionation. Reviews in Mineralogy and Geochemistry, 82(1), 759-798.

Nielsen, S.G., Prytulak, J., Blusztajn, J., Shu, Y., Auro, M., Regelous, M., Walker, J. (2017b). Thallium isotopes as tracers of recycled materials in subduction zones: Review and new data for lavas from Tonga-Kermadec and Central America. Journal of Volcanology and Geothermal Research, 339, 23-40. doi: 10.1016/j.jvolgeores.2017.04.024

Nielsen, S.G., Shu, Y., Wood, B.J., Blusztajn, J., Auro, M., Norris, C.A., Wörner, G. (2021). Thallium Isotope Fractionation During Magma Degassing: Evidence From Experiments and Kamchatka Arc Lavas. Geochemistry, Geophysics, Geosystems, 22, e2020GC009608. https://doi.org/10.1029/2020GC009608

Nobre Silva, I. G., Weis, D., Barling, J., & Scoates, J. S. (2009). Leaching systematics and matrix elimination for the determination of high-precision Pb isotope compositions of ocean island basalts. Geochemistry, Geophysics, Geosystems, 10, Q08012. https://doi.org/10.1029/2009GC002537

Nobre Silva, I. G., Weis, D., & Scoates, J. S. (2013). Isotopic systematics of the early Mauna Kea shield phase and insight into the deep mantle beneath the Pacific Ocean. Geochemistry, Geophysics, Geosystems, 14, 659–676. https://doi.org/10.1002/ggge.20047

Norman, M.D. and Garcia, M.O. (1999) Primitive magmas and source characteristics of the Hawaiian plume: petrology and geochemistry of shield picrites. Earth and Planetary Science Letters, 168, 27-44.

Parai, R., Mukhopadhyay, S., Tucker, J. M. & Pető, M. K. The emerging portrait of an ancient, heterogeneous and continuously evolving mantle plume source. Lithos 346–347, 105153 (2019).

Peacock, C.L., Moon E.M. (2012) Oxidative scavenging of thallium by birnessite: controls on thallium sorption and stable isotope fractionation in marine ferromanganese precipitates. Geochim. Cosmochim. Acta 84, 297–313.

Pietruszka, A. J., Norman, M. D., Garcia, M. O., Marske, J. P., & Burns, D. H. (2013). Chemical heterogeneity in the Hawaiian mantle plume from the alteration and dehydration of recycled oceanic crust. Earth and Planetary Science Letters, 361, 298–309. https://doi.org/10.1016/j.epsl.2012.10.030

Pietruszka, A.J., Marske, J.P., Heaton, D.E., Garcia, M.O., Rhodes, J.M. (2018). An isotopic perspective into the magmatic evolution and architecture of the rift zones of Kīlauea Volcano. J. Pet. 59(12), 2311-2352.

Prytulak, J., Brett, A., Webb, M., Plank, T., Rehkämper, M., Savage, P.S., & Woodhead, J. (2017). Thallium elemental behavior and stable isotope fractionation during magmatic processes. Chemical Geology, 448, 71-83.

Regelous, M., Hofmann, A. W., Abouchami, W., & Galer, S. J. G. (2003). Geochemistry of lavas from the Emperor Seamounts, and the geochemical evolution of Hawaiian magmatism from 85 to 42 Ma. Journal of Petroleum, 44, 113–140.

Rehkämper, M., and Halliday, A.N. (1999) The precise measurement of Tl isotopic compositions by MC-ICP-MS: Application to the analysis of geological materials and meteorites. Geochimica et Cosmochimica Acta, 63, 935-944.

Rehkämper, M., Frank, M., Hein, J. R., Porcelli, D., Halliday, A., Ingri, J., & Liebetrau, V. (2002). Thallium isotope variations in seawater and hydrogenetic, diagenetic, and hydrothermal ferromanganese deposits. Earth and Planetary Science Letters, 197(1), 65-81.

Ren, Z-Y., Takahashi, E., Orihashi, Y., Johnson, K.T.M. (2004). Petrogenesis of Tholeiitic Lavas from the Submarine Hana Ridge, Haleakala Volcano, Hawaii. Journal of Petrology, 45(10), 2067-2099.

Rhodes, J.M. and Vollinger, M.J. (2004). Composition of basaltic lavas sampled by phase-2 of the Hawaii Scientific Drilling Project: Geochemical stratigraphy and magma types. Geochem. Geophys. Geosyst. 5(3), Q03G13.

Schudel, G., Lai, V., Gordon, K., Weis, D. (2015). Trace element characterization of USGS reference materials by HR-ICP-MS and Q-ICP-MS. Chemical Geology, 410, 223-236.

Schiano, P., Dupré, B., Lewin, E. (1993). Application of element concentration variability to the study of basalt alteration (Fangataufa atoll, French Polynesia). Chemical Geology, 104, 99-124.

Shu, Y., Nielsen, S.G., Zeng, Z., Shinjo, R., Blusztajn, J., Wang, X., & Chen, S. (2017). Tracing subducted sediment inputs to the Ryukyu arc-Okinawa Trough system: Evidence from thallium isotopes. Geochimica et Cosmochimica Acta, 217, 462-491.

Starkey, N.A., Jackson, C.R.M., Greenwood, R.C., Parman, S., Franchi, I.A., Jackson, M., Fitton, J.G., Stuart, F.M., Kurz, M., Larsen, L.M. (2016). Triple oxygen isotope composition of the high-^{3}He/4He mantle. Geochimica et Cosmochimica Acta, 176, 227-238. doi: 10.1016/j.gca.2015.12.027

Sun, D., Helmberger, D., Lai, V., Gurnis, M., Jackson, J., Yang, H. (2019). Slab Control on the Northeastern Edge of the Mid-Pacific LLSVP Near Hawaii. Geophys. Res. Lett. 46(6), 3142-3152.

Tanaka, R., Makishima, A., Nakamura, E. (2008). Hawaiian double volcanic chain triggered by and episodic involvement of recycled material: constraints from temporal Sr-Nd-Hf-Pb isotopic trend of the Loa-type volcanoes. Earth Planet. Sci. Lett. 265, 450-465.

Tatsumoto, M. (1978). Isotopic composition of lead in oceanic basalt and its implication to mantle evolution. Earth and Planetary Science Letters, 38(1), 63–87. https://doi.org/10.1016/0012-821X(78)90126-7

Torsvik, T.H., Steinberger, B., Ashwal, L.D., Doubrovine, P.V., Trønnes, R.G. (2016). Earth evolution and dynamics – a tribute to Kevin Burke. Can. J. Earth Sci. 53, 1073–1087. doi: 10.1139/cjes-2015-0228

Weis, D., Kieffer, B., Maerschalk, C., Pretorius, W., Barling, J. (2005). High-precision Pb-Sr-Nd-Hf isotopic characterization of USGS BHVO-1 and BHVO-2 reference materials. Geochem. Geophys. Geosyst., 6, Q02002, doi:10.1029/2004GC000852.

Weis, D., Garcia, M. O., Rhodes, J. M., Jellinek, M., & Scoates, J. S. (2011). Role of the deep mantle in generating the compositional asymmetry of the Hawaiian mantle plume. Nature Geoscience, 4(12), 831–838. https://doi.org/10.1038/ngeo1328

Weis, D., Harrison, L.N., McMillan, R., Williamson, N.M.B. (2020). Fine-scale structure of Earth's deep mantle resolved through statistical analysis of Hawaiian basalt geochemistry. Geochemistry, Geophysics, Geosystems, 21, e2020GC009292. https://doi.org/10.1029/2020GC009292

White, W.M. (1985). Sources of oceanic basalts: Radiogenic isotopic evidence. Geology, 13, 115-118.

White, W.M. (2015). Probing the Earth's deep interior through geochemistry. Geochemical Perspectives, 4, 95–251. https://doi.org/10.7185/ geochempersp.4.2

Williams, C.D., Li, M., McNamara, A.K., Garnero, E.J., van Soest, M.C. (2015). Episodic entrainment of deep primordial mantle material into ocean island basalts. Nat. Comm. 6, 8937-8942.

Williamson, N.M.B., Weis, D., Scoates, J.S., Pelletier, H., & Garcia, M.O. (2019). Tracking the geochemical transition between the Kea-dominated Northwest Hawaiian Ridge and the bilateral Loa-Kea trends of the Hawaiian Islands. Geochemistry, Geophysics, Geosystems, 20 https://doi.org/10.1029/2019GC008451

Wilson, S.A. (1997). The collection, preparation and testing of USGS reference material BCR-2, Columbia River, Basalt, U.S. Geological Survey Open-File Report 98-00x.

Woodhead, J.D., Greenwood, P., Harmon, R.S., Stoffers, P. (1993). Oxygen isotope evidence for recycled crust in the source of EM-type ocean island basalts. Nature, 362, 809-813.

Zindler, A., & Hart, S. R. (1986). Chemical geodynamics. Annual Review of Earth and Planetary Sciences, 14(1), 493–571. https://doi.org/10.1146/annurev.earth.14.1.493

References from Supporting Information

Broadley, M.W., Sumino, H., Graham, D.W., Burgess, R., Ballentine, C.J. (2018). Recycled components in mantle plumes deduced from variations in halogens (Cl, Br, and I), trace elements, and $^{3}He/^{4}He$ along the Hawaiian-Emperor seamount chain. Geochemistry, Geophysics, Geosystems, 20, 277-294. doi: 10.1029/2018GC00795

Fitton, J. G., Saunders, A.D., Norry, M.J., Hardarson, B.S., Taylor, R.N. (1997). Thermal and chemical structure of the Iceland plume, Earth and Planetary Science Letters, 153, 197–208, doi:10.1016/S0012-821X(97)00170-2.

Garcia, M.O., Caplan-Auerbach, J., De Carlo, E.H., Kurz, M.D., Becker, N. (2006). Geology, geochemistry and earthquake history of Lo‘ihi Seamount, Hawai‘i’s youngest volcano. Chem. Erde 66, 81-108.

Garcia, M. O., Swinnard, L., Weis, D., Greene, A. R., Gami, T., Sano, H., & Gandy, C. E. (2010). Petrology, geochemistry and geochronology of Kaua'i lavas over 4·5 Myr: Implications for the origin of rejuvenated volcanism and the evolution of the Hawaiian plume. Journal of Petrology, 51(7), 1507–1540. https://doi.org/10.1093/petrology/egq027

Kurz, M.D., Jenkins, W.J., Hart, S.R., Clague, D. (1983). Helium isotopic variations in volcanic rocks from Loihi Seamount and the Island of Hawaii. Earth Planet. Sci. Lett. 66, 388-406.

Mukhopadhyay, S., Lassiter, J. C., Farley, K. A., & Bogue, S. W. (2003). Geochemistry of Kauai shield-stage lavas: Implications for the chemical evolution of the Hawaiian plume. Geochemistry, Geophysics, Geosystems, 4(1), 1009. https://doi.org/10.1029/2002GC000342

1083 **Tables**
1084

Table 1
Tl concentrations and isotopic compositions of reference materials, duplicates, and replicates[1]

Reference material	Volcano	Pre-treatment for isotopes	Sample type	Tl (ng/g)	ε^{205}Tl	2SD[2]	Measurements (n)
BCR-2 U	Columbia River basalt	Unleached	Subaerial	307	-2.4	0.4	33
BCR-2 U REP					*-2.5*	*0.7*	*3*
BCR-2 L	Columbia River basalt	Leached	Subaerial	281	-2.3	0.7	3
BCR-2 L DUP					*-2.4*	*0.1*	*3*
BCR-2 L REP[4]					*-2.3*	*0.4*	*2*
BHVO-1 U	Kīlauea	Unleached	Subaerial	45	-3.6	0.4	1
BHVO-1 L	Kīlauea	Leached	Subaerial	17	-3.6	0.8	3
BHVO-2 U	Kīlauea	Unleached	Subaerial	23	-1.3	0.5	3
BHVO-2 L	Kīlauea	Leached	Subaerial	16	-1.5	0.3	3
KIL-93 U	Kīlauea	Unleached	Subaerial	19	*-1.9*	*0.4*	*1*
KIL-93 U DUP[3]					*-2.2*	*0.4*	*1*
KIL-93 L	Kīlauea	Leached	Subaerial	16	-1.0	0.4	2
KIL-93 L DUP					*-1.6*	*0.5*	*3*
KOOLAU U	Koʻolau	Unleached	Subaerial	22	-1.7	0.4	1
KOOLAU L	Koʻolau	Leached	Subaerial	9	-2.6	0.4	2

[1]Tl isotopic compositions were measured on a *Nu Plasma* MC-ICP-MS from leached (L) or unleached (U) whole rock powders that were purified twice by ion exchange chromatography. Data were corrected for internal mass fractionation using Pb standard NIST NBS 981, details in text. Average $^{205}Tl/^{203}Tl$ obtained for NIST SRM 997 during this study is 2.38913 ± 0.00040, RSD of 167 ppm (n = 609) and for the Aldrich standard is 2.38894 ± 0.00037, RSD of 154 ppm (n = 100).
[2]2SD is the external uncertainty of the individual sample measurements reported to the significant digit. When only one or two measurements were possible (n = 1 or 2), the average long-term reproducibility of leached reference materials (2SD of 0.4) is used.
[3]DUP = Procedural duplicate of the same sample. Values are italicized.
[4]REP = Replicate MC-ICP-MS analysis of the same sample solution. Values are italicized.

1085

Table 2
Tl isotopic compositions, and Tl and Ce concentrations, for Hawaiian samples and their duplicates[1]

Sample ID	Volcano	Hawaiian geochemical group	Pre-treatment for isotopes	Sample type	Ce µg/g	Tl ng/g	ε^{205}Tl	2SD[2]	Measurements (n)
P287-1 L	Lōʻihi	Loa	Leached	Submarine	29.3	21	-1.8	0.4	2

186-3 L	Lōʻihi	Loa	Leached	Submarine	24.7	18	-2.1	0.4	2
KS11-1 (1954) L	Kīlauea	Kea	Leached	Subaerial	40.3	26	-0.5	0.4	2
K88-20 (1921-4) L	Kīlauea	Kea	Leached	Subaerial	37.5	23	-1.6	0.4	2
UB-15 L	Kīlauea	Kea	Leached	Subaerial	30.2	19	-1.7	0.4	2
KIL-93 L	Kīlauea	Kea	Leached	Subaerial	30.0	19	-1.3	0.6	5
ML-95 L	Mauna Loa	Loa	Leached	Subaerial	21.7	38	-2.3	0.3	3
L00-003-11 L	Mauna Loa	Loa	Leached	Subaerial	22.4	14	-1.6	0.4	2
J2-019-08 L	Mauna Loa	Loa	Leached	Submarine	13.0	10	-1.9	0.2	3
J2-019-019 L	Mauna Loa	Loa	Leached	Submarine	21.6	19	-1.5	0.4	1
J2-019-019 L DUP[3]							*-1.6*	*0.4*	*2*
R154-2.1-2.95 L	Mauna Kea	Kea	Leached	Core	19.7	14	-1.3	0.4	2
R187-0.9-2.5 L	Mauna Kea	Kea	Leached	Core	21.1	14	-2.8	0.4	2
R219-5.5-7.7 L	Mauna Kea	Kea	Leached	Core	28.7	20	-1.6	0.4	2
SR0871-13.00 L	Mauna Kea	Kea	Leached	Core	23.0	14	-1.1	0.3	3
KK-9-2 L	Hualālai	Loa	Leached	Submarine	23.0	17	-1.7	0.3	3
KK-78-12-11-1 L	Hualālai	Loa	Leached	Submarine	14.7	12	-1.5	0.4	2
MG-4A L	Kohala	Kea	Leached	Subaerial	56.6	19	-0.7	0.4	2
K212-8 L	Hāna Ridge (Haleakalā)	Kea	Leached	Submarine	35.6	263	2.0	0.4	2
K214-3 L	Hāna Ridge (Haleakalā)	Kea	Leached	Submarine	13.7	26	-1.5	0.4	2
01-MA-560 L	West Maui	Kea	Leached	Core	36.0	13	1.8	0.4	2
01-MA-560 L DUP							*2.0*	*0.4*	*3*
01-MA-1020 L	West Maui	Kea	Leached	Core	49.9	18	0.9	0.4	2
00-OL-33a L	West Maui	Kea	Leached	Subaerial	27.6	7.2	-2.8	0.2	3
02-WA-10 L	West Maui	Kea	Leached	Subaerial	39.1	8.7	-1.0	0.4	2
00-LP-01 L	West Maui	Kea	Leached	Subaerial	51.7	11	-2.6	0.4	2
KOOLAU L	Koʻolau	Enriched Loa	Leached	Subaerial	30.3	22	-2.6	0.4	2
WH-182 L	Koʻolau	Enriched Loa	Leached	Core	31.7	23	-2.1	0.4	2
WH-489 L	Koʻolau	Enriched Loa	Leached	Core	40.3	22	-2.2	0.4	1
WH-360 L	Koʻolau	Enriched Loa	Leached	Core	33.9	22	-2.6	0.3	3
WA-2017-09 L	Waiʻanae	Loa	Leached	Subaerial	37.3	28	-1.6	0.4	2
WA-2017-09 L DUP							*-1.4*	*0.4*	*2*
J2-306-15 L	West Kaʻena	Loa	Leached	Submarine	20.7	24	-2.1	0.4	2
J2-305-4 L	West Kaʻena	Loa	Leached	Submarine	24.5	87	-1.2	0.4	1
J2-306-11 L	West Kaʻena	Loa	Leached	Submarine	9.6	11	-1.4	0.4	3
KAU-2015-017 L	Kauaʻi	Loa	Leached	Subaerial	27.6	15	-2.4	0.4	2
KAU-2015-026 L	Kauaʻi	Kea	Leached	Subaerial	29.1	9.4	4.0	0.4	2

[1]Tl isotopic compositions were measured on a *Nu Plasma* MC-ICP-MS from leached (L) or unleached (U) whole rock powders that were purified twice by ion exchange chromatography. (L) or (U) designations do not apply here to trace elements - for those, see Appendix 1. Isotopic data were corrected for internal mass fractionation using Pb standard NIST NBS 981, details in text. Average $^{205}Tl/^{203}Tl$ obtained for NIST SRM 997 during this study is 2.38913 ± 0.00040, RSD of 167 ppm (n = 609) and for the Aldrich standard is 2.38894 ± 0.00037, RSD of 154 ppm (n = 100).
[2]2SD is the external uncertainty of the individual sample measurements reported to the significant digit. When only one or two measurements were possible (n = 1 or 2), the average long-term reproducibility of leached reference materials (2SD of 0.4) is used.
[3]DUP = Procedural duplicate of the same sample, values are italicized. For replicate information see supporting information Table S1.

Figure captions

Figure 1. Map and Pb-Pb plot for Hawaiian volcanoes showing samples used in this study. (a) Map of the Hawaiian volcanoes and Loa-Kea geographic and geochemical trends, modified from Williamson et al. (2019). Samples analyzed in this study are indicated and are coloured according to the legend in (b). Inset shows present-day plume cross-section with Loa (blue) and Kea (red) compositional domains indicated. White arrow inside the cross-section indicates both the compositional boundary within the plume as well as the current direction of Pacific plate motion (northwest). (b) Plot of $^{206}Pb/^{204}Pb$ vs. $^{208}Pb/^{204}Pb$ showing a compilation of high-precision data for shield-stage Hawaiian lavas. Division between Loa and Kea samples is represented by the black line and was calculated by Abouchami et al. (2005). Hawaiian Pb isotope dataset is available from Williamson et al. (2019) for Kauaʻi and Waiʻanae volcanoes and Weis et al. (2020) for all other volcanoes. The Pb data for samples used in this study are included in supporting Tables S1 and S2.

Figure 2. Thallium concentrations and isotopic compositions in Hawaiian lavas. (a) Tl (ng/g) vs $\varepsilon^{205}Tl$ coloured by geochemical group (Kea, Loa, Enriched Loa, left plot) and by volcano (right plot). Empty squares represent previous data (unleached) and filled circles represent current data (leached). Error bars on previous and current $\varepsilon^{205}Tl$ values are 2SD and in some cases are smaller than symbol size. (b) Box plots of $\varepsilon^{205}Tl$, and $^{208}Pb^*/^{206}Pb^*$ for comparison (insets), for the three major Hawaiian geochemical groups (Kea, Loa, Enriched Loa) and the six subgroups (Average Loa, Enriched Loa, Kea, Transitional Kea, Kohala, Lōʻihi) recently defined by Weis et al. (2020). Lines in $^{208}Pb^*/^{206}Pb^*$ plots designate division between Loa compositions (above) and Kea (below), after Abouchami et al. (2005). In all box plots, the numbers next to middle lines are the medians. Boxes are set to IQR = inter-quartile range, which is the difference between the 1st and 3rd quartile (the entire box represents 3rd minus 1st). Thus, the lowest box line represents the 1st quartile and the top box line represents the 3rd quartile. Data outliers are designated by circle symbols outside of the box whiskers: filled symbols are 1.5x outside the IQR and open symbols are 3x outside the IQR. Whiskers represent the smallest and largest non-outliers.

Figure 3. Trace element plots for Hawaiian samples compared to $\varepsilon^{205}Tl$. Legend is the same as in Figure 2a. (a) Ce/Tl compared to $\varepsilon^{205}Tl$ with negative trend for West Maui samples indicated by green arrow, and Cs/Tl (b), Pb/Tl (c), and Rb/Tl (d) compared to $\varepsilon^{205}Tl$. Grey bands in (a) and (b) represent typical mantle values. Trace element data is available in Tables S1.

Figure 4. Plots of Th, Ce, and Ce/Tl vs. $^{208}Pb^*/^{206}Pb^*$ for the Hawaiian samples analysed. Legend is the same as Fig. 2a, with volcanoes organized by Loa or Kea geochemical group.

Figure 5. Plots of Th/Rb vs. Ce/Tl, $\varepsilon^{205}Tl$ vs. Rb/Cs, $\varepsilon^{205}Tl$ vs Th/Tl, and $\varepsilon^{205}Tl$ vs. Ba/Rb for the Hawaiian samples analysed. Legend is same as in Fig. 2a. When error bars are not visible for $\varepsilon^{205}Tl$ they are smaller than symbol size.

Figure 6. Thallium isotopic compositions in Hawaiian lavas compared to radiogenic isotopes. Shown are comparisons with $^{208}Pb^*/^{206}Pb^*$, $^{206}Pb/^{204}Pb$, $^{87}Sr/^{86}Sr$, and $^{176}Hf/^{177}Hf$ and legend is the same as in Figure 2a. Note that two samples used in the current study do not have Sr isotopic data and six do not have Hf isotopic data – these were not included in our additional radiogenic isotopic analyses due sample availability. Error bars on $\varepsilon^{205}Tl$ values are 2SD and in some cases are smaller than symbol size. Line in $^{208}Pb^*/^{206}Pb^*$ plot designates the division between Loa and Kea compositions after Abouchami et al. (2005). Included in the radiogenic Pb and Sr plots are previous data for four subaerial samples from Nielsen et al. (2006b). Isotopic data for all Hawaiian samples can be found in Table S1 and S2.

Figure 7. (a) Plot shows calculated volcano means of $\varepsilon^{205}Tl$ (this study, n = 34, Table 1) versus $\delta^{18}O$ (literature data measured in olivine, n = 138, Table S3). Means, indicated by star symbols, are coloured for Loa (blue), Enriched Loa (dark blue), and Kea (red) according to their radiogenic Pb values (e.g., Figure 1 and 3). Background fields are coloured blue for Loa-trend volcanoes and red for Kea-trend volcanoes. Note that some volcanoes do not have data for both $\varepsilon^{205}Tl$ and $\delta^{18}O$. For example, O isotopic data exist for the Enriched Loa volcano of Lana‘i but no samples from this volcano were analyzed for $\varepsilon^{205}Tl$ and so they are not included in this plot. Note also that Haleakalā and Hāna Ridge are part of the same volcanic system – Hāna Ridge is the eastern submarine rift of the Haleakalā volcano and forms part of its shield-building volcanic stage (Ren et al., 2004). The Kaua‘i symbol is uncolored because it is not known whether the O data is from west or east Kaua‘i – this determines whether they belong to the Loa or Kea group (Williamson et al., 2019; Weis et al., 2020), and although we are reasonably confident that they are west Kaua‘i samples, and therefore Kea, we cannot be absolutely certain. This is illustrated by the dotted line that extends the red Kea field towards Kaua‘i. Two black lines represent $\delta^{18}O$ values for average mantle (bottom line, 5.2‰; Mattey et al., 1994) and average MORB (top line, 5.5‰ ;Eiler 2001). (b) Box plots of $\delta^{18}O$ data for Hawaiian volcanoes with insets showing $\varepsilon^{205}Tl$ for comparison. Legend is indicated and is the same as in Figure 2. See Figure 2 for box plot explanation and description of outlying data. Note that no $\delta^{18}O$ data from the literature are available for Lō‘ihi.

Figure 1.

(a)

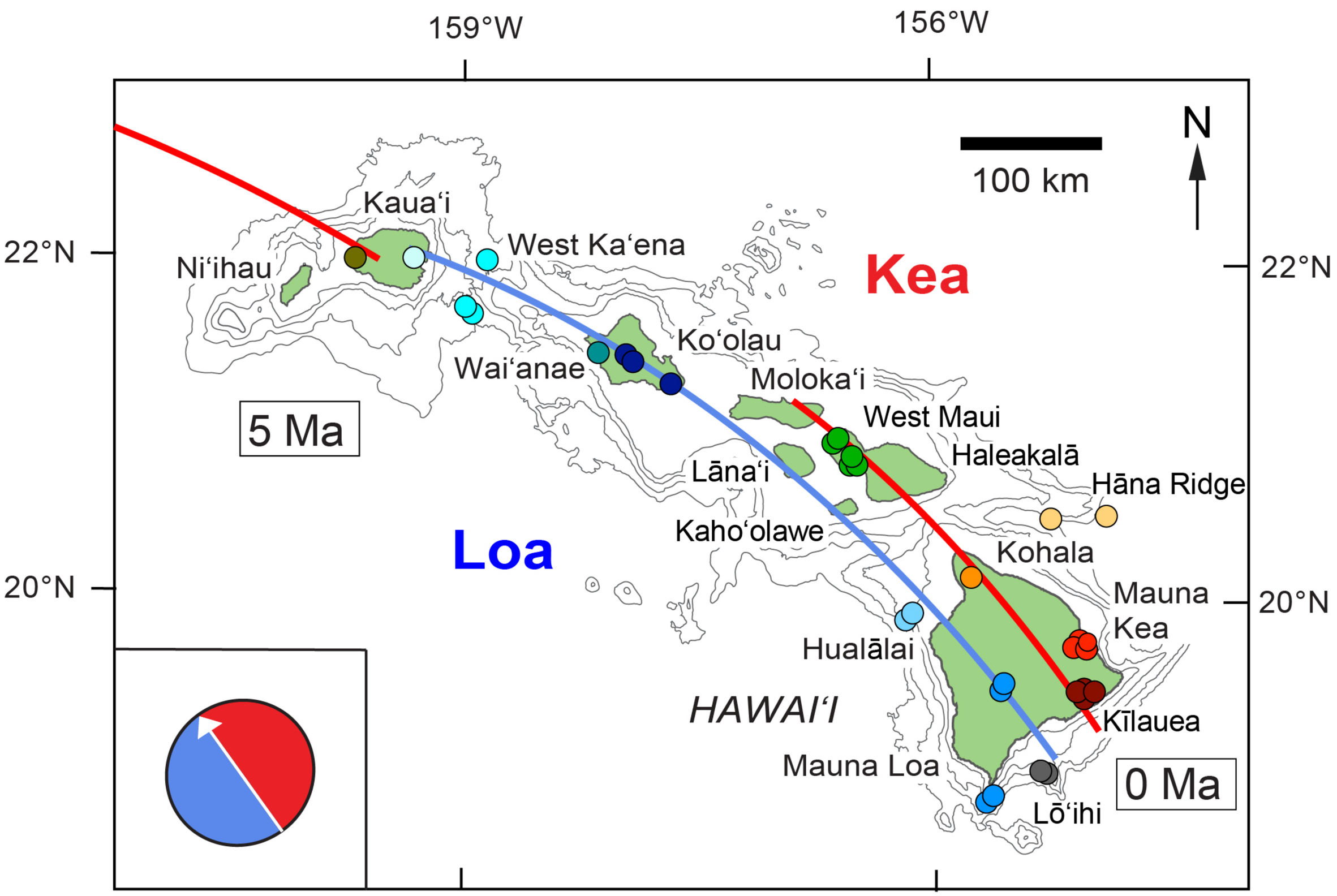
159°W
156°W
22°N
20°N
N
100 km
Kaua‘i
Ni‘ihau
West Ka‘ena
Kea
Ko‘olau
Wai‘anae
Moloka‘i
West Maui
Haleakalā
Lāna‘i
Hāna Ridge
Kaho‘olawe
Kohala
Loa
Mauna Kea
Hualālai
HAWAI‘I
Kīlauea
Mauna Loa
Lō‘ihi
5 Ma
0 Ma

(b)

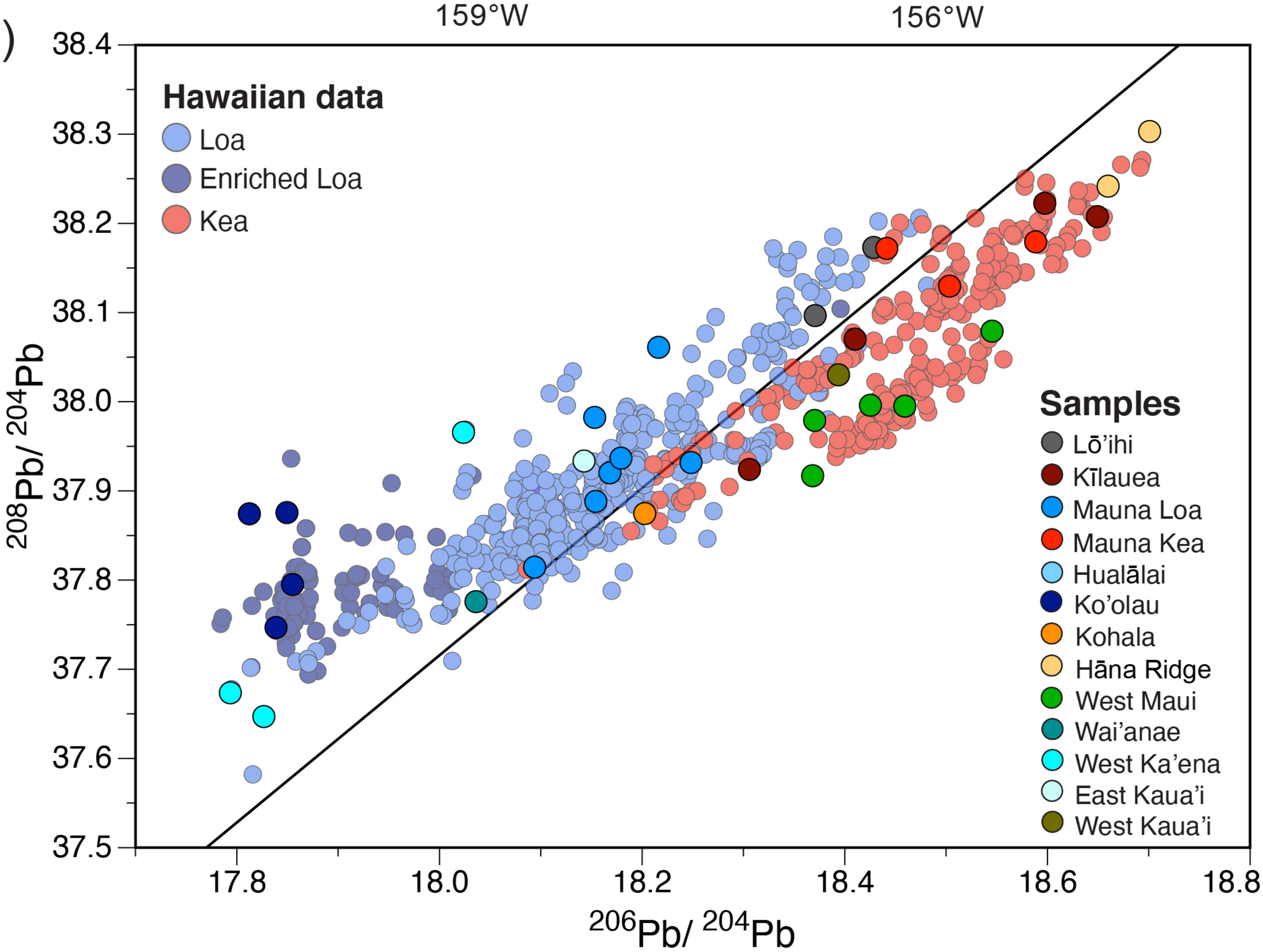
Hawaiian data
Loa
Enriched Loa
Kea
Samples
Lō’ihi
Kīlauea
Mauna Loa
Mauna Kea
Hualālai
Ko’olau
Kohala
Hāna Ridge
West Maui
Wai’anae
West Ka’ena
East Kaua’i
West Kaua’i
38.4
38.3
38.2
38.1
38.0
37.9
37.8
37.7
37.6
37.5
17.8
18.0
18.2
18.4
18.6
18.8
208Pb/ 204Pb
206Pb/ 204Pb

Figure 2.

(a)

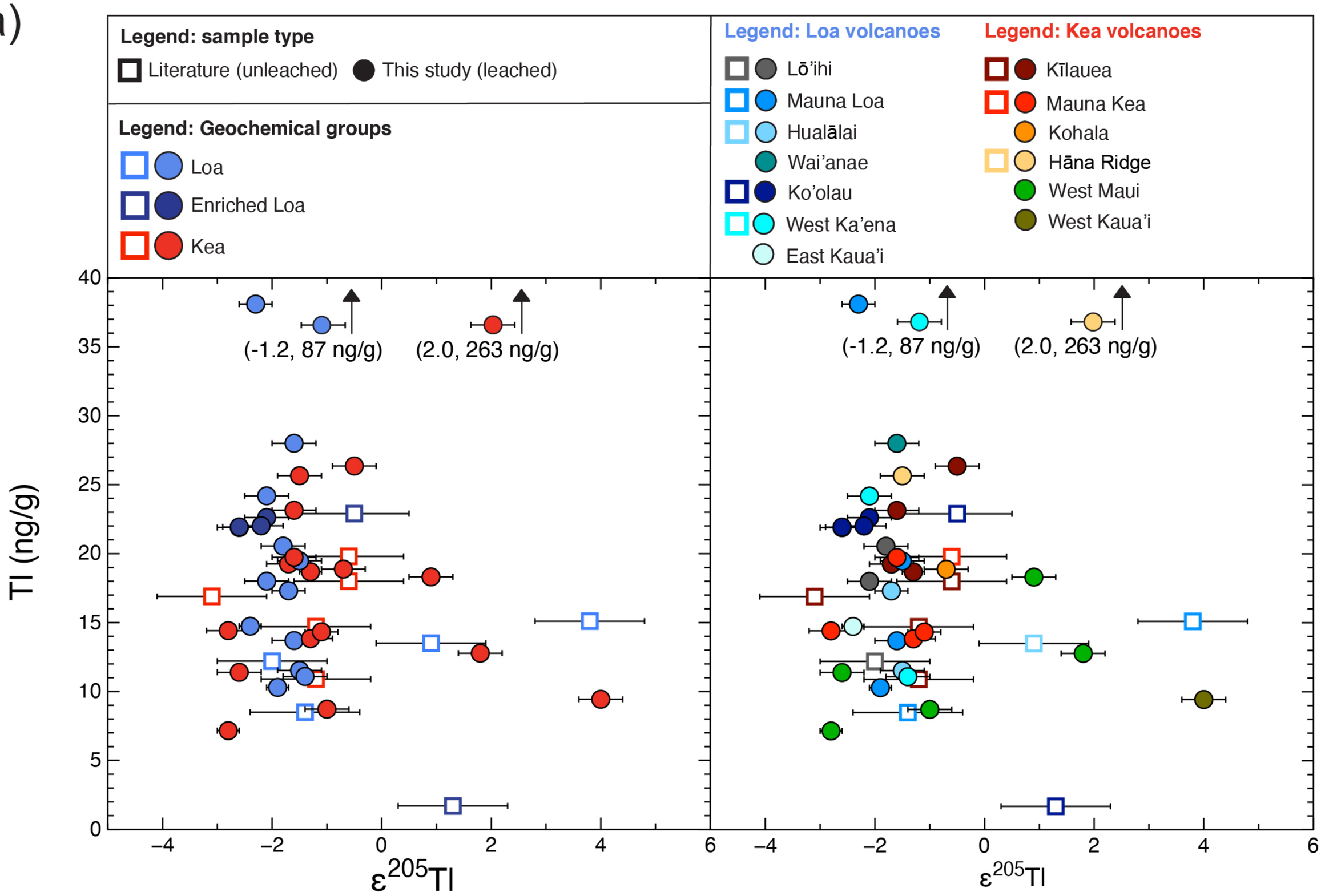
Legend: sample type
Literature (unleached)
This study (leached)
Legend: Geochemical groups
Loa
Enriched Loa
Kea
Legend: Loa volcanoes
Lō'ihi
Mauna Loa
Hualālai
Wai'anae
Ko'olau
West Ka'ena
East Kaua'i
Legend: Kea volcanoes
Kīlauea
Mauna Kea
Kohala
Hāna Ridge
West Maui
West Kaua'i
(-1.2, 87 ng/g)
(2.0, 263 ng/g)
Tl (ng/g)
ε205Tl
ε205Tl

(b)

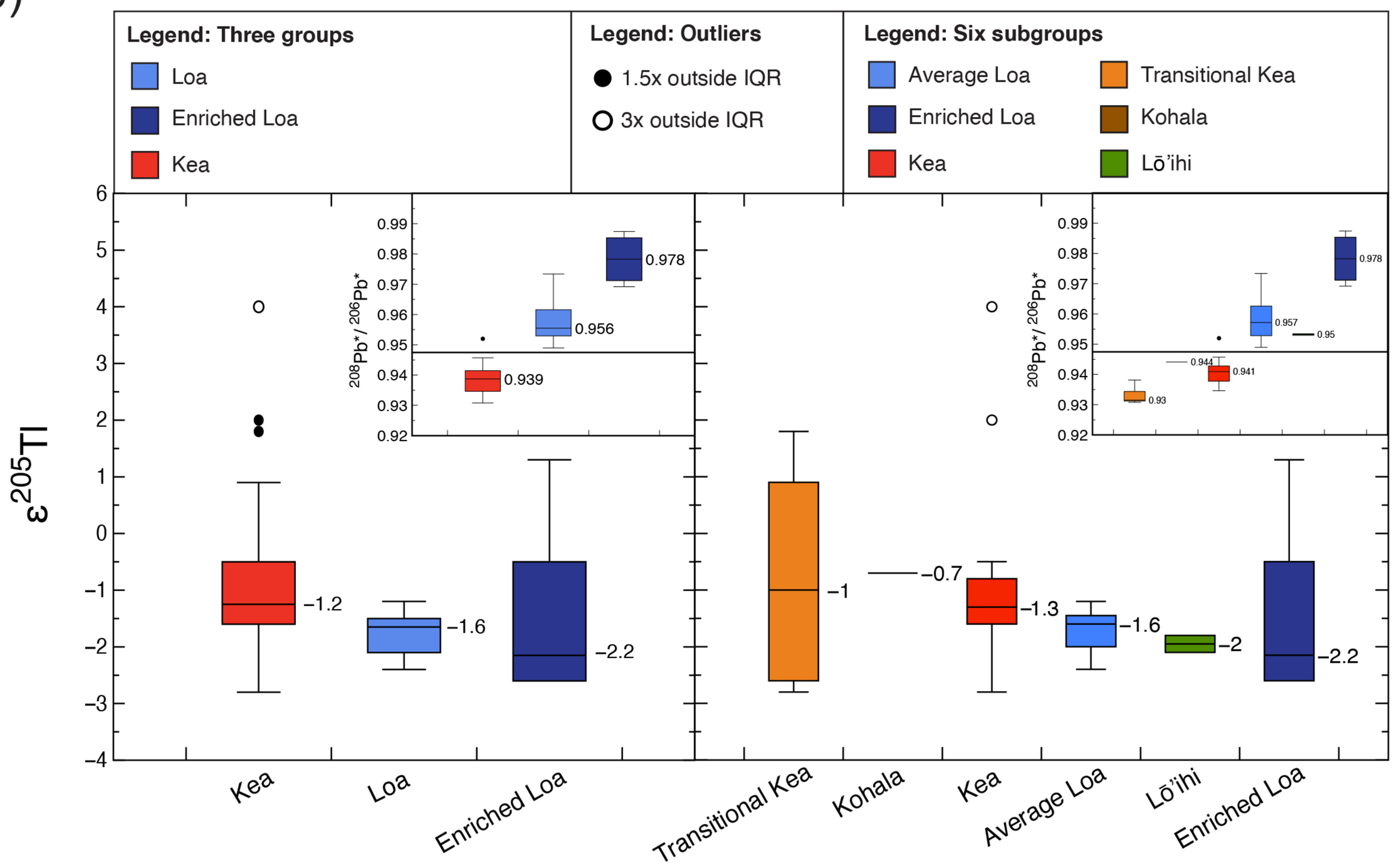
Legend: Three groups
Loa
Enriched Loa
Kea
Legend: Outliers
1.5x outside IQR
3x outside IQR
Legend: Six subgroups
Average Loa
Enriched Loa
Kea
Transitional Kea
Kohala
Lō'ihi
208Pb*/206Pb*
0.939
0.956
0.978
0.93
0.944
0.941
0.957
0.95
0.978
ε205Tl
−1.2
−1.6
−2.2
−1
−0.7
−1.3
−1.6
−2
−2.2
Kea
Loa
Enriched Loa
Transitional Kea
Kohala
Kea
Average Loa
Lō'ihi
Enriched Loa

Figure 3.

(a)

(b)

(c)

(d)

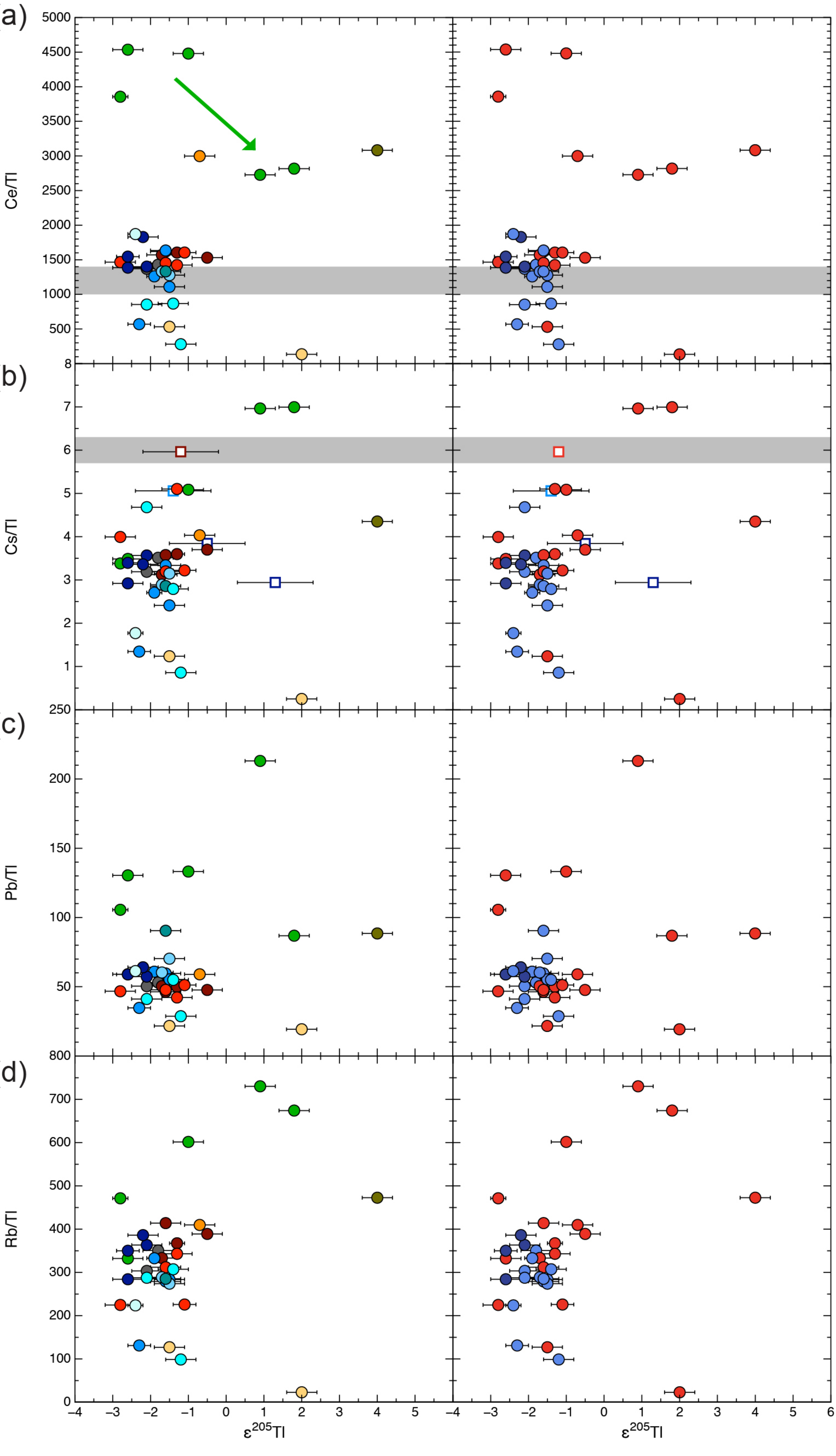

Figure 4.

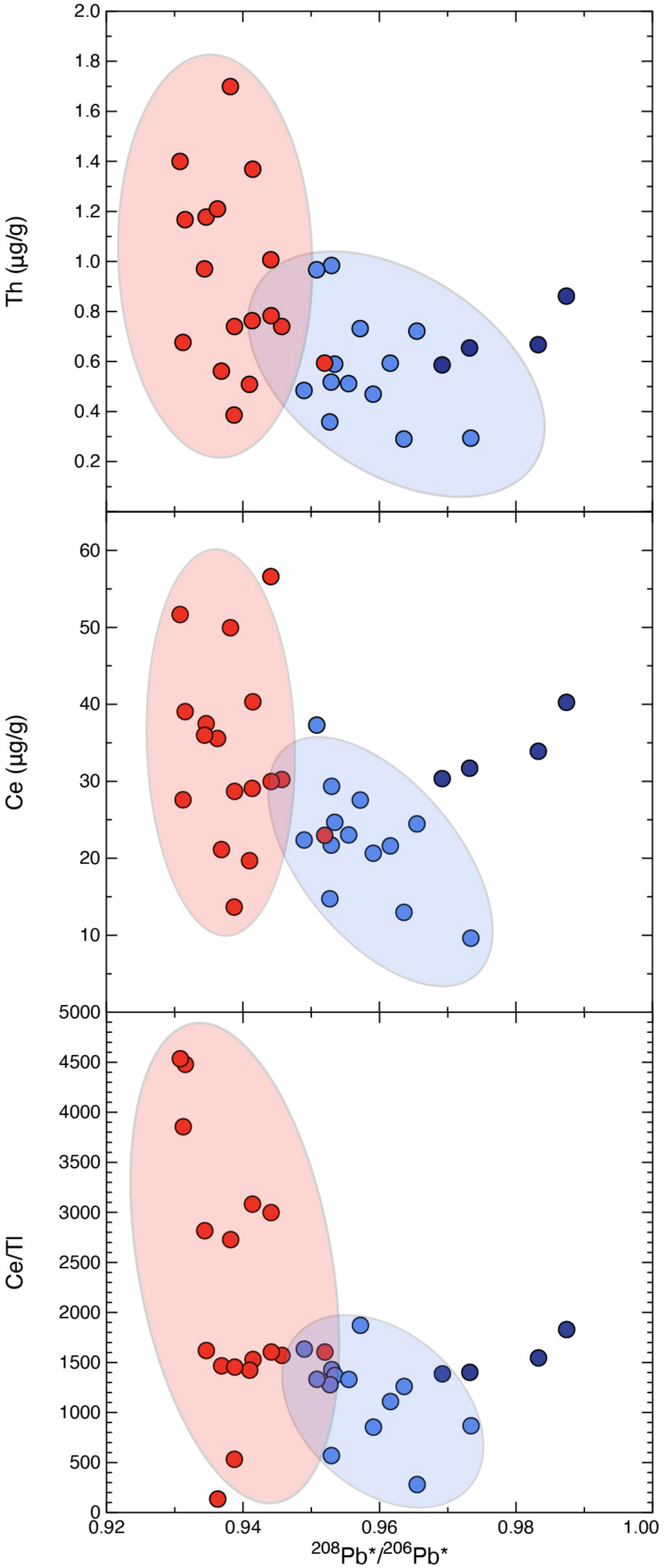
Th (µg/g)
2.0
1.8
1.6
1.4
1.2
1.0
0.8
0.6
0.4
0.2
Ce (µg/g)
60
50
40
30
20
10
5000
Ce/Tl
4500
4000
3500
3000
2500
2000
1500
1000
500
0
0.92
0.94
0.96
0.98
1.00
$^{208}Pb^*/^{206}Pb^*$

Figure 5.

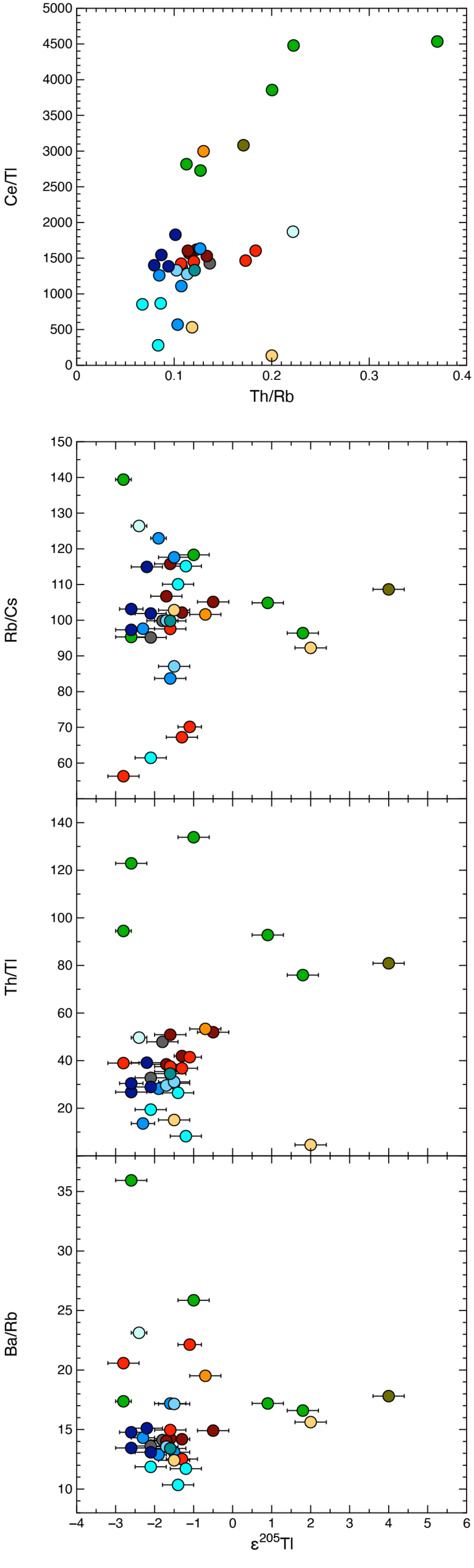
Ce/Tl
Th/Rb
Rb/Cs
Th/Tl
Ba/Rb
ε205Tl

Figure 6.

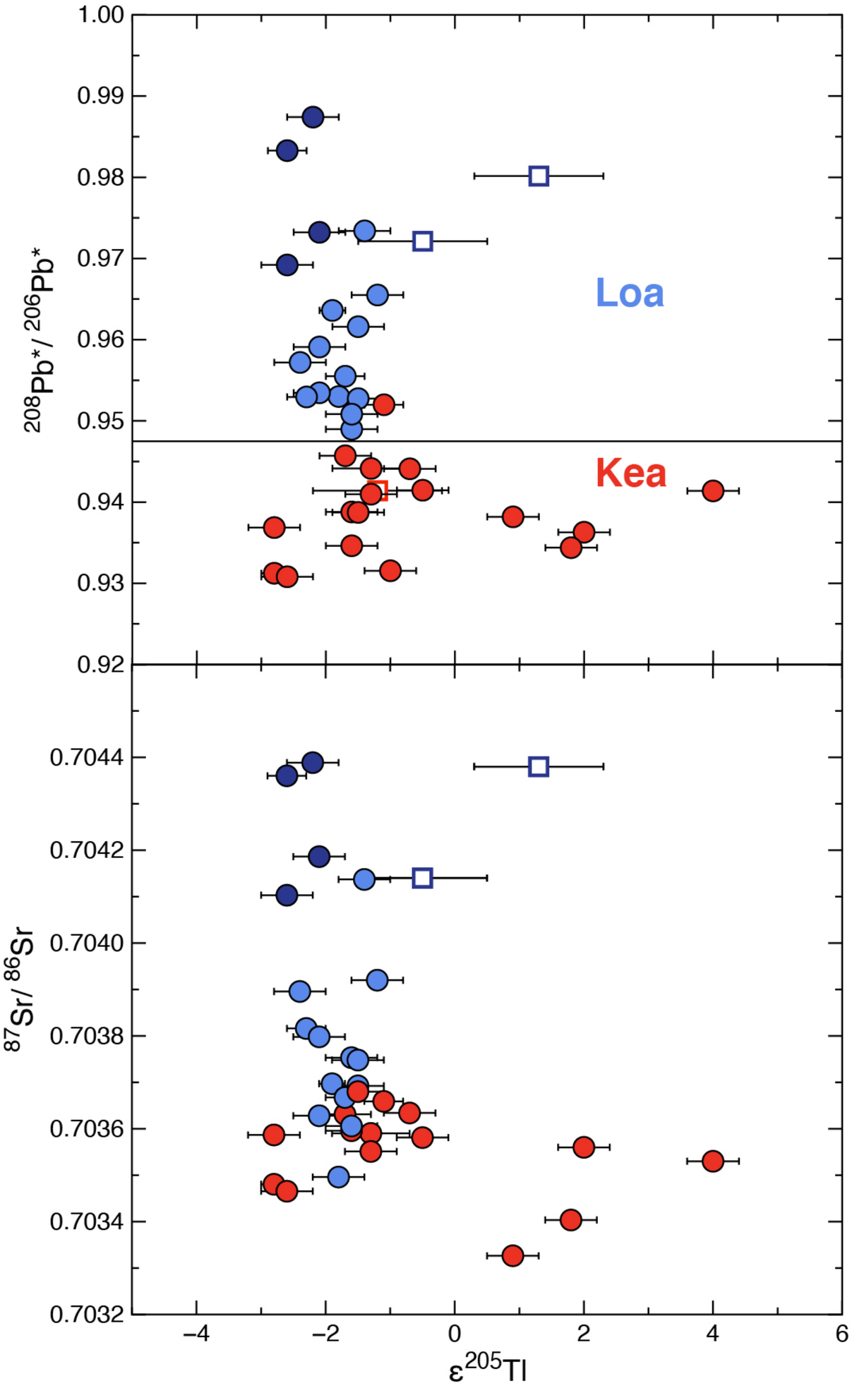
Loa
Kea
208Pb*/206Pb*
87Sr/86Sr
ε205Tl
1.00
0.99
0.98
0.97
0.96
0.95
0.94
0.93
0.92
0.7044
0.7042
0.7040
0.7038
0.7036
0.7034
0.7032
−4
−2
0
2
4
6

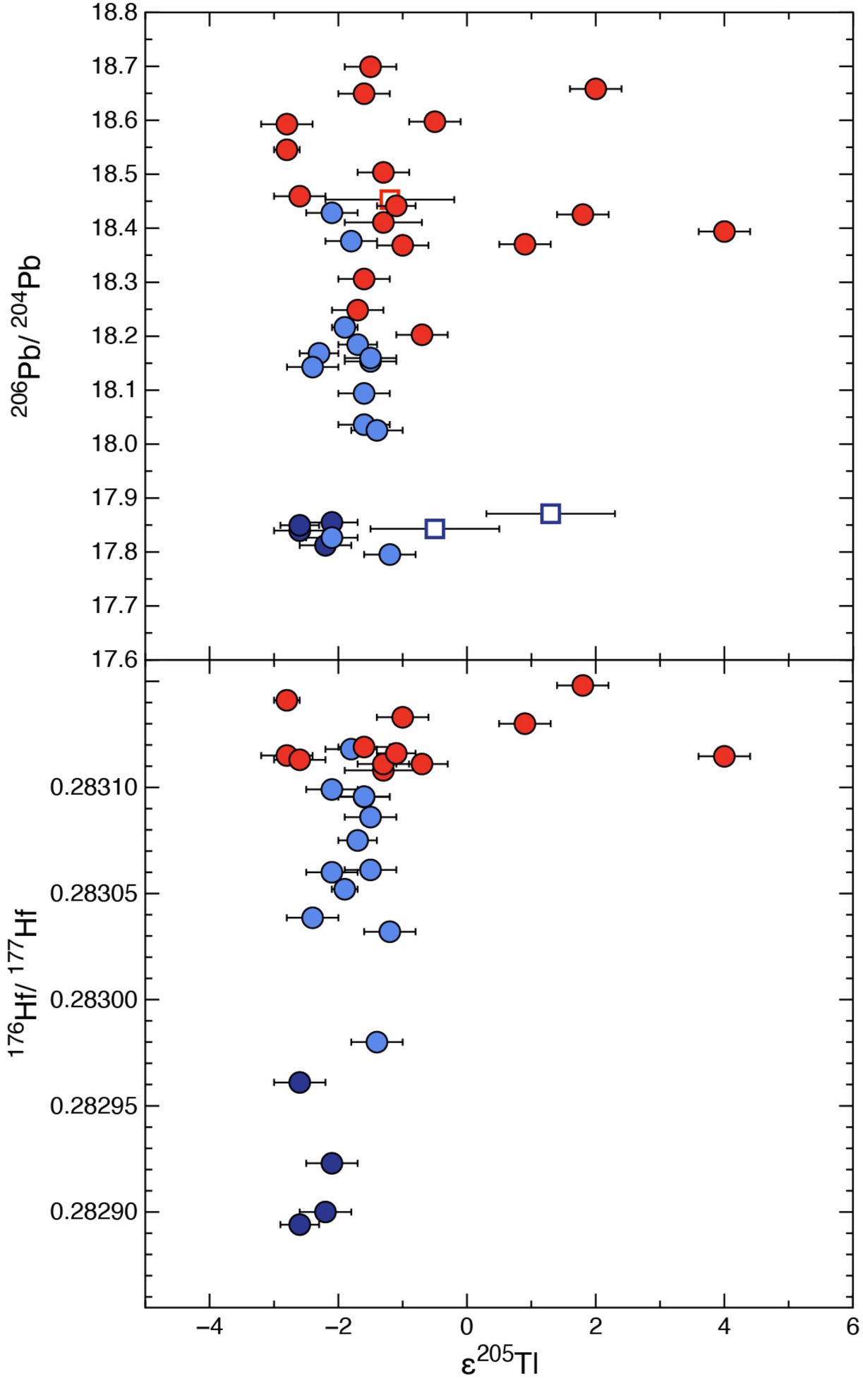
206Pb/204Pb
176Hf/177Hf
ε205Tl
18.8
18.7
18.6
18.5
18.4
18.3
18.2
18.1
18.0
17.9
17.8
17.7
17.6
0.28310
0.28305
0.28300
0.28295
0.28290
−4
−2
0
2
4
6

Figure 7.

(a)

Legend: Geochemical groups and data type

- Loa
- Enriched Loa
- Kea
- Means from this study (Tl) and literature (O), by volcano

Legend: volcano abbreviations

- ML: Mauna Loa
- H: Hualālai
- Ko: Ko'olau
- K: Kīlauea
- MK: Mauna Kea
- Kh: Kohala
- HR: Haleakalā/Hāna Ridge
- Kau: Kaua'i

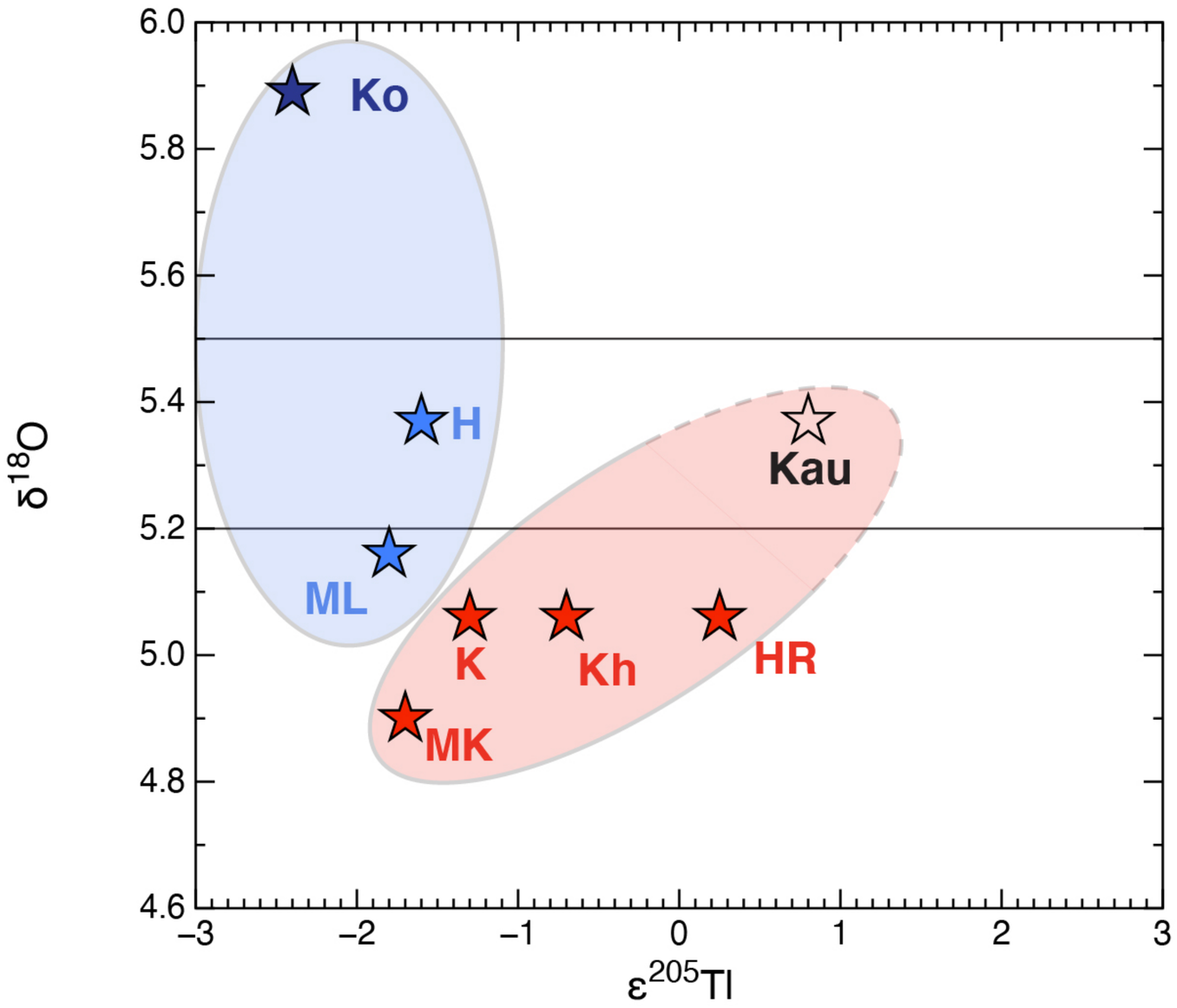

(b)

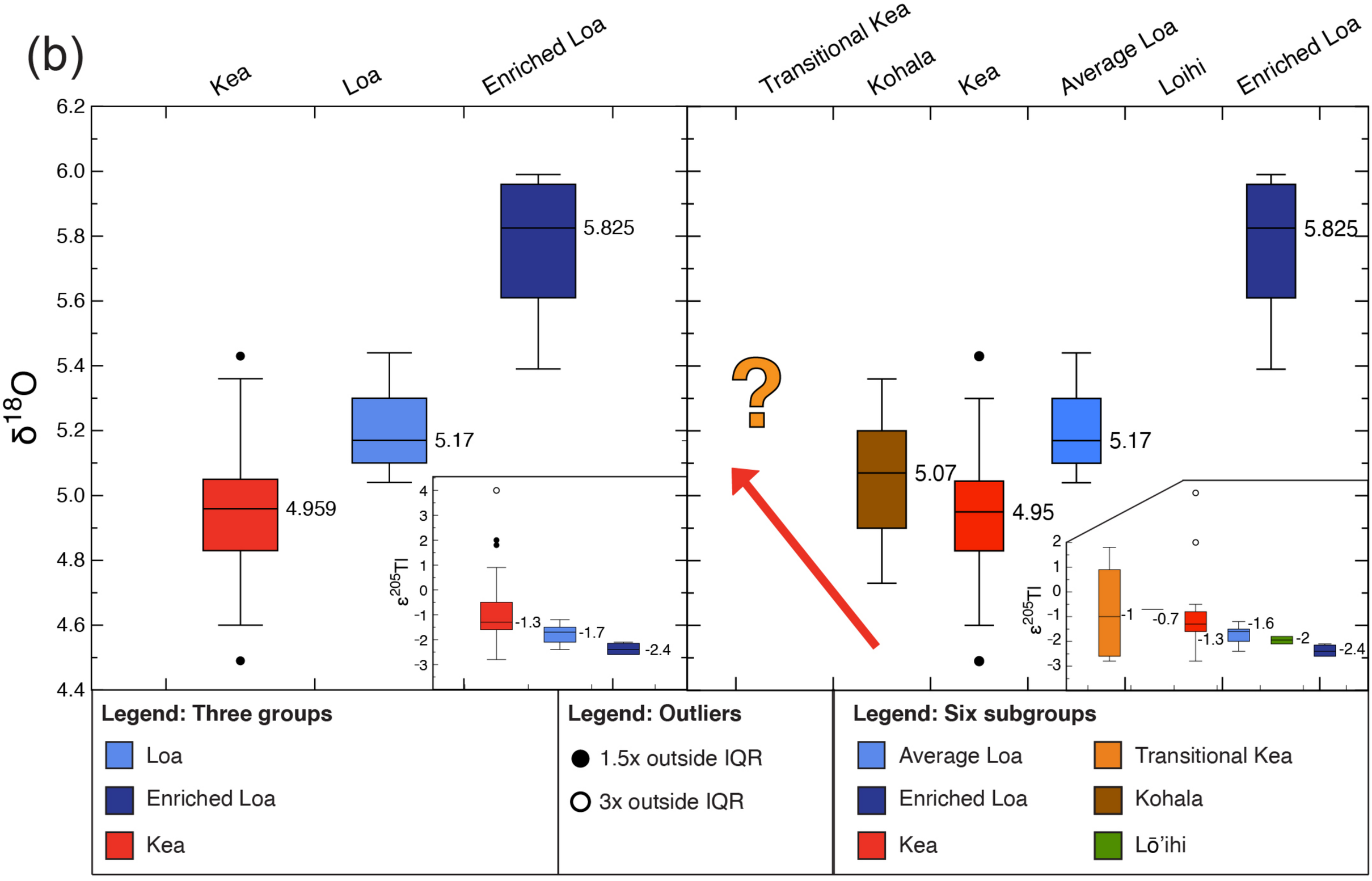

Legend: Three groups

- Loa
- Enriched Loa
- Kea

Legend: Outliers

- 1.5x outside IQR
- 3x outside IQR

Legend: Six subgroups

- Average Loa
- Enriched Loa
- Kea
- Transitional Kea
- Kohala
- Lō'ihi